博 士 論 文
（Doctoral Thesis）

Understanding aspects behind recombination-dependent telomere maintenance and chromosome circularization using fission yeast

（分裂酵母を用いた環状染色体と組換え依存テロメア維持に関する性質の理解）

Ahmed Gamal Kamel Habib

広島大学大学院先端物質科学研究科

（Graduate School of Advanced Sciences of Matter
Hiroshima University）

2018 年 3 月
（March 2018）

目　　次
（Table of Contents）

主　論　文
(Main Thesis)

Abstract

Telomeres are nucleoprotein structure located in the extremities of linear chromosomes to maintain the integrity of chromosome ends. Telomere dysfunction is one of the key driving forces for genomic instability and cancers. For instance, recombination-dependent telomere maintenance and chromosome circularization following telomere dysfunction had been reported in association with cancers. Identifying vulnerable points in these two telomere dysfunction cases would help find a possible target for cancer therapy.

The fission yeast *Schizosaccharomyces pombe* provides an excellent model for studying telomere maintenance due to the ease of genetic manipulation and the conservation of many telomere-related genes from yeast to human. In fission yeast, deletion of *pot1*$^{+}$, which encodes for protection of telomere 1, results in rapid telomere loss and chromosome circularization, a phenotype resembles cancer cells with circular chromosomes. Fission yeast Rqh1 is a member of the RecQ helicase family that regulates homologous recombination (HR) events. The *pot1*Δ *rqh1-hd* (helicase dead) double mutant maintains telomeres by HR and recombination intermediates accumulate at telomeres of the double mutant. Moreover, *pot1*Δ *rqh1-hd* cells display long G2 phase and sensitive to microtubule inhibitor thiabendazole (TBZ).

One purpose of my research is to understand the mechanism of the TBZ sensitivity phenotype of the *pot1*Δ *rqh1-hd* double mutant which may allow me to find a specific vulnerability in cancer cells that maintain telomeres by HR. Interestingly, I found that shortening the G2 of the *pot1*Δ *rqh1-hd* double mutant by concomitant loss-of-function mutation of DNA damage checkpoint proteins Wee1 and Mik1 or gain-of-function mutation of Cdc2 (*cdc2-3w*) suppressed the TBZ sensitivity and the

accumulation of recombination intermediates at chromosome ends of the *pot1*Δ *rqh1-hd* double mutant. My results suggest that the activation of DNA damage checkpoint signaling and holding the *pot1*Δ *rqh1-hd* cells at long G2 provide time for the accumulation of toxic recombination structures at chromosome ends which perturb chromosome segregation and render cells sensitive to TBZ. My results further imply that elongation of G2 phase and inhibition of resolution of recombination intermediate may sensitize cancer cells that maintain telomere by recombination to anti-microtubule drugs.

The second purpose of my research is to identify the gene required for the maintenance of the circular chromosome using fission yeast *pot1*Δ cells. This gene could be a target of cancer therapy that specifically kills cancer cells that have circular chromosomes. To date, the mechanisms behind the maintenance of circular chromosomes and how cells with circular chromosomes could survive are largely enigmatic. I found that the lack of function of chromosome passenger complex (CPC) is lethal to cells with circular chromosomes, demonstrating the importance of CPC for the survival of cells with circular chromosomes and shedding light on the possible role of CPC in the maintenance of circular chromosomes.

Together, my work proves that fission yeast is a good model organism to understand the mechanism of genome stability and cancer-related phenotypes that would directly contribute to cancer therapy and possibly other human diseases.

Contents

Organization of the thesis

Chapter 1. Provides a general introduction and background about telomere, RecQ helicases, and ring chromosomes and their implication in genetic diseases and cancers with a brief introduction of the model organism used in this study, the fission yeast *S. pombe*, and the aim of the thesis.

Chapter 2. Describes a study of the correlation between long G2 phenotype of *S. pombe pot1*Δ *rqh1-hd* double mutant and its sensitivity to microtubule inhibitor thiabendazole (TBZ). I demonstrated how the activation of DNA damage checkpoint pathway and holding the *pot1*Δ *rqh1-hd* cells at long G2 render cells sensitive to TBZ.

Chapter 3. Characterizes the importance of chromosome passenger complex (CPC) for the survival of cells with ring chromosomes using a synthetic lethality approach. I demonstrated that functional CPC is required for the survival of fission yeast cells with circular chromosomes. In addition, the synthetic lethality phenotype of CPC dysfunction in cells with ring chromosomes is discussed.

Finally, **Chapter 4**. Provides a conclusion of the thesis, thesis achievements and the potential future perspectives of the thesis.

Chapter 1. Introduction

1.1 Telomeres: structure and function

The term telomere stems from the Greek word as “telos” means “end” and “meros” means “part” referring to a structure located at the termini of linear chromosomes. The first attempts to realize that the end of linear chromosomes has unique features stemmed from the experiments done by Herman Muller and Barbara McClintock. By using the fruit fly *Drosophila melanogaster*, Muller observed that the ends of chromosomes are almost stable and did not show genetic alteration such as deletion or inversion upon irradiation of chromosomes with X-ray [1]. McClintock observed a variable behavior of broken chromosomes and telomeres using *Zea mays* [2]. Meanwhile, broken chromosomes were able to fuse together; telomeric DNA did not. Further work on telomeres was done by Elizabeth Blackburn and Joseph Gall using the single-celled organism, *Tetrahymena thermophila* which has the advantage of containing thousands of minichromosomes, providing sufficient telomeric materials to be studied [3]. Later, a collaborative work between Blackburn and Jack Szostak demonstrated the presence of telomeres in other organisms such as budding yeast *Saccharomyces cerevisiae* [4]. The importance of the discovery of telomeres and telomerase was realized by the 2009 Nobel Prize to Elizabeth Blackburn, Jack Szostak, and Carol Greider for the discovery of how chromosomes are protected by telomeres [5]. Since that time, many model organisms have been exploited to understand the molecular biology of telomeres and its implication in human diseases.

In general, telomeres are DNA/protein complex located at the termini of linear chromosomes composed of double-stranded DNA repeat sequences followed by single-

stranded G-rich overhang at the 3′ terminus known as “G-tail”, a structure that marks the chromosome ends from the other parts of the genome [6]. The G-tail is presumed to form because of resection of the 5′ end of the C-strand and present in all organisms studied so far with variable length among organisms [7]. The length of telomeres varies from one organism to another. For instance, human telomeres are 10-20 kb long [8], while both fission yeast and budding yeast have a telomere length of 300 bp [9, 10]. Laboratory mouse and rats’ telomeres extend to a range of 20-50 kb [11]. A known exception is *Drosophila melanogaster* in which telomeres consist of arrays of telomere-specific non-long terminal repeat retrotransposons [12]. The telomeric repeat sequences are largely evolutionarily conserved among species. The telomeres in human composed of hexameric repeat sequence of $(TTAGGG)_n$ [13], in *Tetrahymena* $(TTGGGG)_n$ [14], in *Oxytricha* $(TTTTGGGG)_n$ [15], and in plants $(TTTAGGG)_n$ [16], except for the alga *Chlamydomonas* which uses $(TTTTAGGG)_n$ [17]. Yeasts have the same general motif for the telomeric sequences with slight diversion. For instance, *Saccharomyces cerevisiae* has $(TG_{1\text{-}3})_n$ sequence, while *Schizosaccharomyces pombe* has $(TTACAG_{1\text{-}8})_n$ [9, 10].

Because of the ability of conventional DNA polymerase to extend DNA only from 5′ to 3′, one of the two DNA strands will be synthesized continuously called “leading strand” whereas the other strand is known as “lagging strand” will be synthesized discontinuously in the form of short DNA segments called “Okazaki fragment” [18]. The DNA polymerase cannot initiate the DNA synthesis directly and needs very short stretches of RNA (RNA primers) to prime each round of DNA synthesis. After the maturation of Okazaki fragments, the RNA segments are removed and replaced by DNA followed by ligation of these DNA segments generating continuous lagging strand. However, the removal of RNA primers at the termini of the

newly synthesized DNA cannot be replenished resulting in loss of the terminal parts of chromosomal DNA with each round of cell cycle, a phenomenon known as "the end-replication problem" which was first proposed by James Watson and Olovnikov (Fig. 1.1) [19, 20]

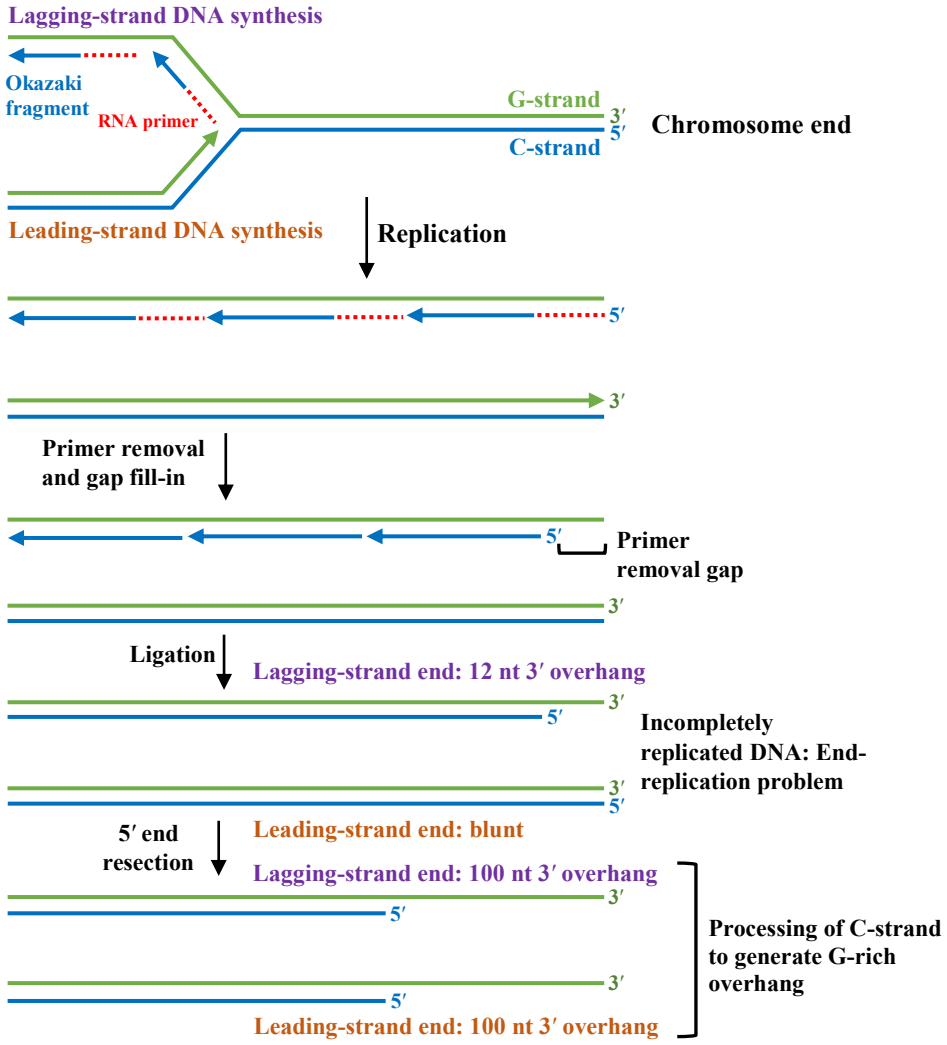

Fig. 1.1. The end-replication problem. The synthesis of DNA is initiated by a stretch of RNA fragment called RNA primer (showed as a dotted line). The DNA polymerase can extend DNA only from 5′ to 3′. Therefore, one of the two strands will be synthesized continuously called "leading strand" whereas the other strand "lagging strand" will be synthesized discontinuously in the form of short DNA segments called "Okazaki fragment." In the absence of telomerase, the removal of RNA primer at the termini of newly synthesized DNA cannot be replenished resulting in loss of the terminal parts of chromosomal DNA with each round of cell cycle. Captured from the work of Wilhelm Palm and Titia de Lange. Annu. Rev. Genet. 2008. 42:301–34.

An enzyme known as telomerase can solve the end-replication problem. Telomerase is a specialized reverse transcriptase that uses its RNA as a template for DNA synthesis [14]. In the absence of telomerase, continuous loss of DNA terminal regions will occur with successive rounds of cell divisions which adversely affects genomic stability in the long term [21]. Telomere shortening with increasing passage number was also observed in vitro in cultured human fibroblast, a phenomenon known as “Hayflick limit” [22].

If the lost telomeric repeats are not replenished, telomeres become very short and sensed as DNA damage (Fig. 1.2) [23]. The activation of DNA damage response halts the cells from further division and leads to senescence known as “replicative senescence” [23]. Therefore, to maintain genome integrity, the chromosome ends must be protected not to be recognized as DNA double-strand break (DSB) and override the DNA repair and DNA damage checkpoint responses. To achieve this, a complex of protein had been identified to bind and protect the telomeric DNA known as “shelterin”. In mammals, the shelterin consists of complex of hexameric proteins; TRF1, TRF2, TIN2, RAP1, TPP1, and POT1 [24, 25] (Fig. 1.3 and 1.4). This shelterin has exquisite binding specificity and mainly present at telomeres and does not exist at any elsewhere in the genome. TFR1 and TRF2 are double-stranded (ds) telomeric binding proteins [26], and POT1 is a single-stranded (ss) telomere-binding protein that binds to the single-stranded overhang [27]. These proteins are held together by TIN2 and TPP1 which act as a bridge that tethers TRF1and TRF2 with POT1 [28]. The fission yeast telomere shelterin consisting of Taz1, Rap1, Poz1, Tpz1, Ccq1, and Pot1 shows a striking similarity to that of a human compared with budding yeast [24, 25]. Taz1, the ortholog of TRF1/2 binds to ds telomeric repeat [29], and Pot1, the ortholog of human POT1, binds to the ss overhang [30] (Fig. 1.3).

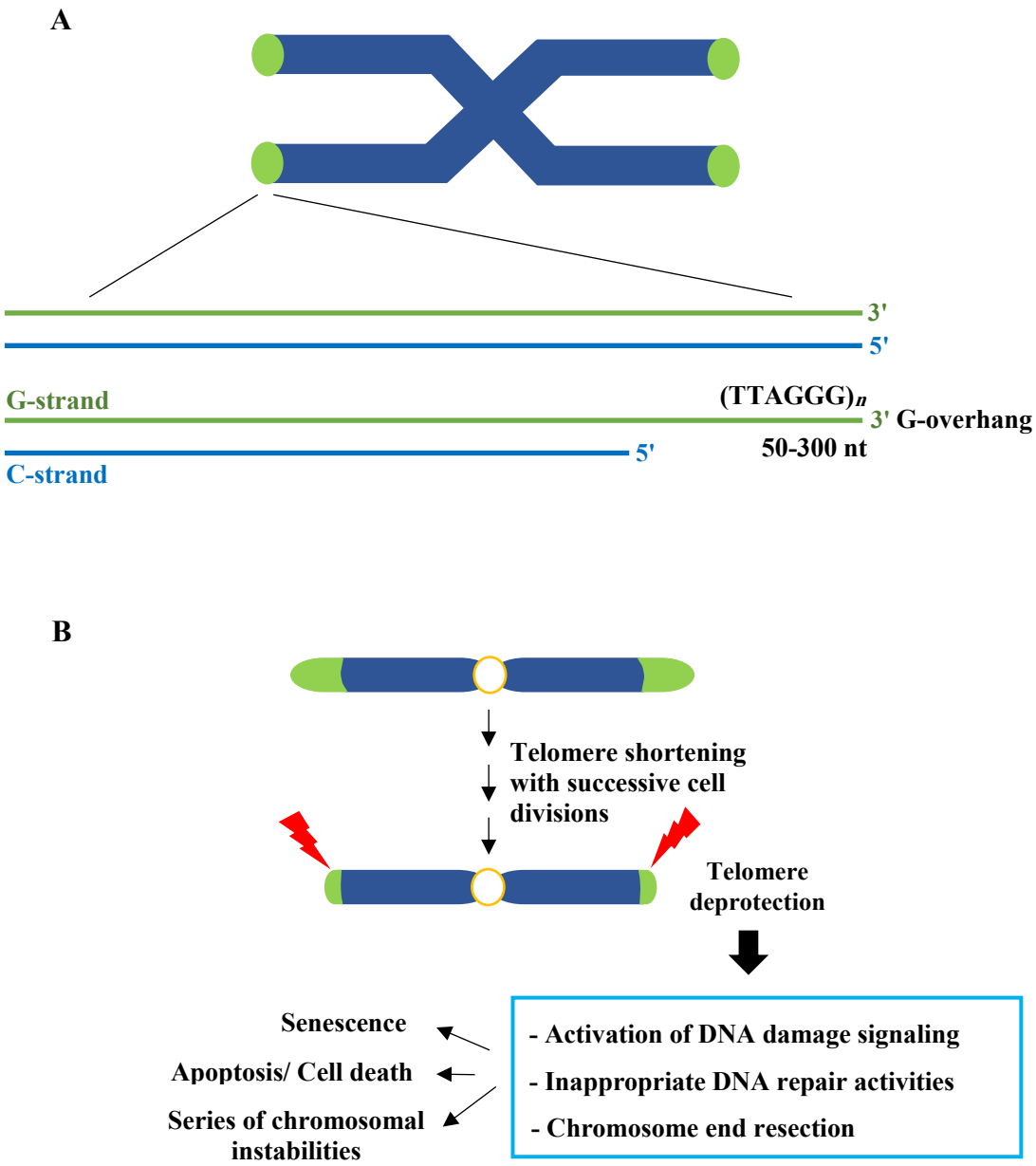

Fig. 1.2 (A) Schematic view of eukaryotic chromosomes. The green region indicates the telomeres. Telomere replication is followed by processing of the 5′ end resulting in the generation of G-rich overhang at the 3′ terminus. (B) Telomere shortening with subsequent cell divisions results in telomere deprotection. Short telomeres are sensed as DNA damage site resulting in activation of DNA damage and DNA repair pathways which could have deleterious consequences on cell fates such as chromosomal instabilities, permanent cell cycle arrest, and cell death.

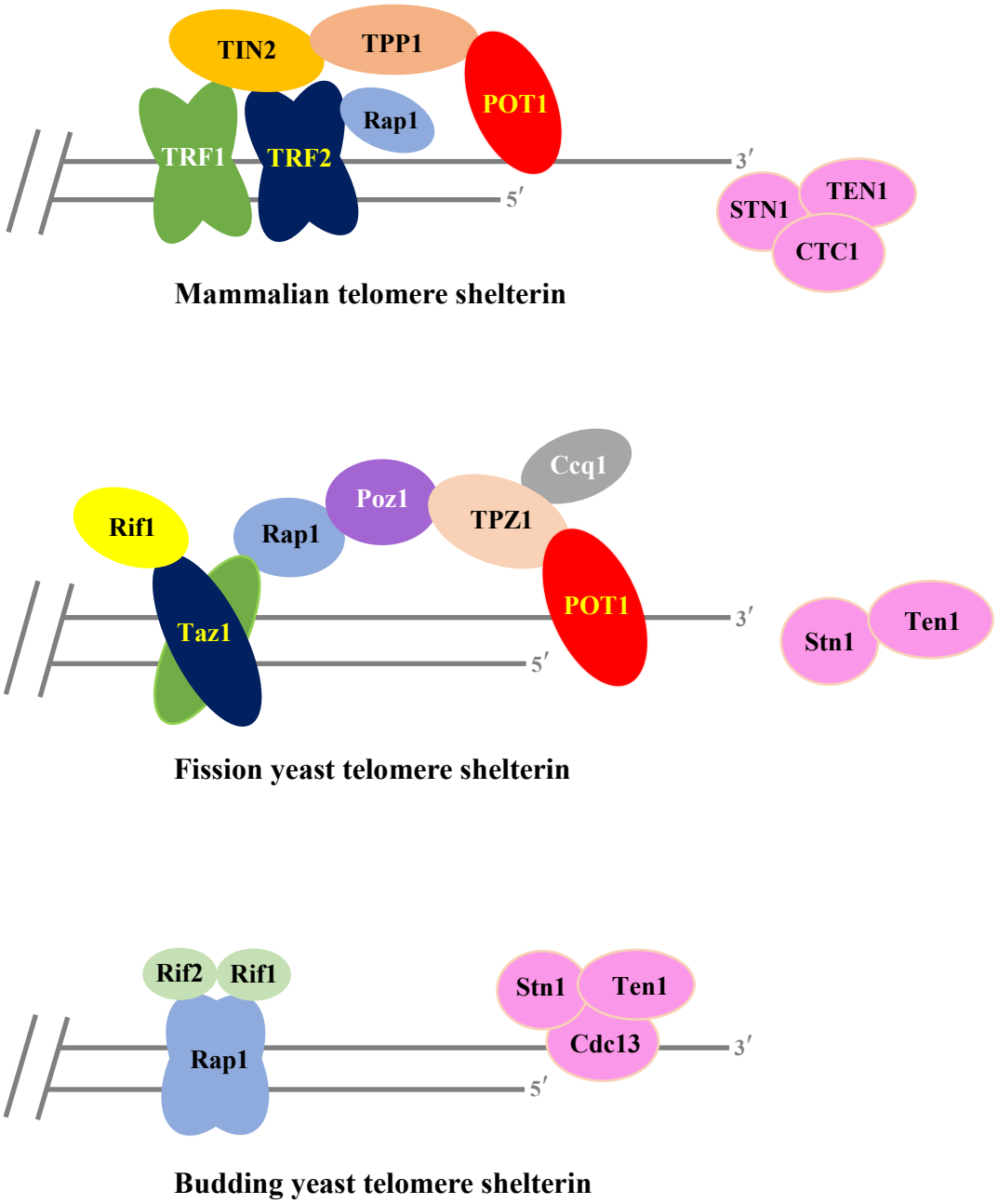

Fig. 1.3. Schematic representation of the conservation of telomere shelterin among different eukaryotes. The fission yeast telomere shelterin closely resembles that of mammals. Fission yeast Taz1 is the ortholog of mammalian TRF1/2 binds to the ds telomeric repeat, and Pot1, the ortholog of human POT1, binds to the ss overhang. Budding yeast lacks TRF1/TRF2 homolog. Instead, Rap1 can bind directly to ds telomeric region. The CST (CTC1–STN1–TEN1) complex then binds to shelterin to facilitate the synthesis of C-strand. Inspired by the work of Jain D and Cooper JP. 2010. Annu Rev Genet 44: 243–269.

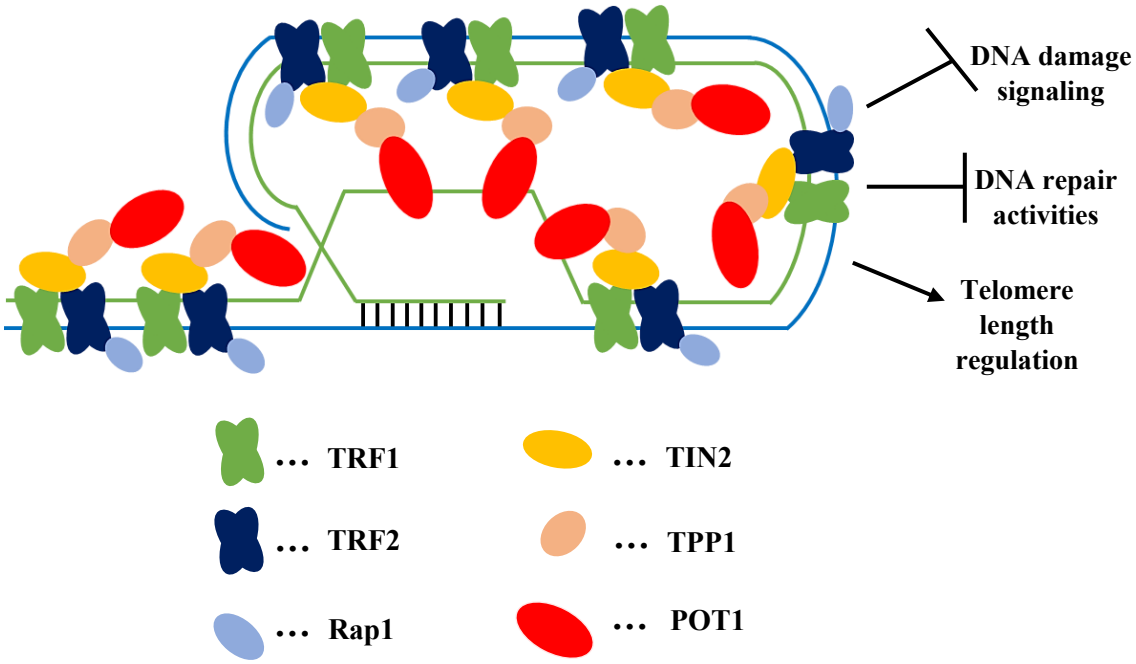

Fig. 1.4. A schematic view of the localization patterns of telomere-binding proteins that shape the telomere shelterin to preserve telomeric integrity. Telomere shelterin protects chromosome ends from being recognized as DNA damage sites and accordingly inhibits the DNA repair pathways such as nonhomologous end joining (NHEJ) and homology-directed repair (HDR) and regulates telomere length.

1.1.1 Telomere dysfunction and cancers

The failure of shelterin to confer their protective role results in telomere dysfunction manifested with variable phenotypes such as telomere shortening, telomere loss, telomere fusion, telomere lengthening, or recombination between telomeric repeats. For instance, deletion of fission yeast *pot1*$^{+}$ or its binding partner *tpz1*$^{+}$ results in immediate telomere loss and cells can only survive through chromosome circularization, suggesting the important function of the Pot1-Tpz1 complex in telomere protection [30, 31]. However, the deletion of *taz1*$^{+}$, *rap1*$^{+}$ or *poz1*$^{+}$ results in telomerase-dependent hyper-elongation of telomeres, implying that these proteins inhibit telomerase recruitment [31, 32].

Telomere dysfunction has been reported to be involved in the aging process and cancers [21]. A detrimental consequence of telomere dysfunction is the end-to-end chromosome fusion which results in the formation of dicentric chromosomes, rings, and sister-chromatid fusion [21] (Fig. 1.5). The segregation of dicentric chromosomes results in anaphase bridge and chromosome breakage followed by a series of chromosomal breakage-fusion-bridge cycles leading to deleterious chromosomal rearrangement and genome instability. POT1 is the first telomere shelterin components whose mutation is linked to human cancers [33-35].

In fact, telomere shortening acts as a double-edged sword. From one side, progressive telomere shortening with cell divisions can eventually lead to replicative senescence which would prevent the progression of pre-malignant cells and thus conferring a tumor suppression mechanism. On the other side, some cells can escape cell senescence and divide indefinitely producing potential tumorigenic cells and enter a state known as “crisis”. Beyond this crisis state, cells undergo a series of genomic instability and chromosome rearrangement which can eventually lead to upregulation of telomerase and indefinite progression of premalignant cells and cancers. Consistently, the majority of cancer cells (85-90%) can circumvent telomere shortening crisis and maintain telomeres through reactivation of telomerase [36]. Telomerase is usually undetectable or present at very low levels in human somatic cells [36]. Nevertheless, a population of cancer cells (10-15%) can continue growing with no detectable level of telomerase and lengthen their telomeres through a pathway known as alternative lengthening of telomeres (ALT) which involves HR between telomeres [37]. Telomerase-independent telomere maintenance through HR has been observed in some organisms such as mosquito, *Anopheles gambiae*, yeasts, and telomerase-null mouse cells [38-41]. The molecular mechanisms underlying the maintenance of

telomeres by ALT remain unknown. Although some telomerase inhibitors have been entered clinical trials, till now, there are no inhibitors of the ALT cancer cells have been developed [42]. This possibly may due to the lack of specific molecules that can target the ALT pathway. Moreover, ALT cancer cells show resistance to treatment with telomerase inhibitors and the treatment of telomerase-positive cancer cells with telomerase inhibitors triggers the transformation of these cells into ALT cells [42]. Therefore, more understanding of recombination-dependent telomere maintenance pathway would have significant implications for cancer therapy.

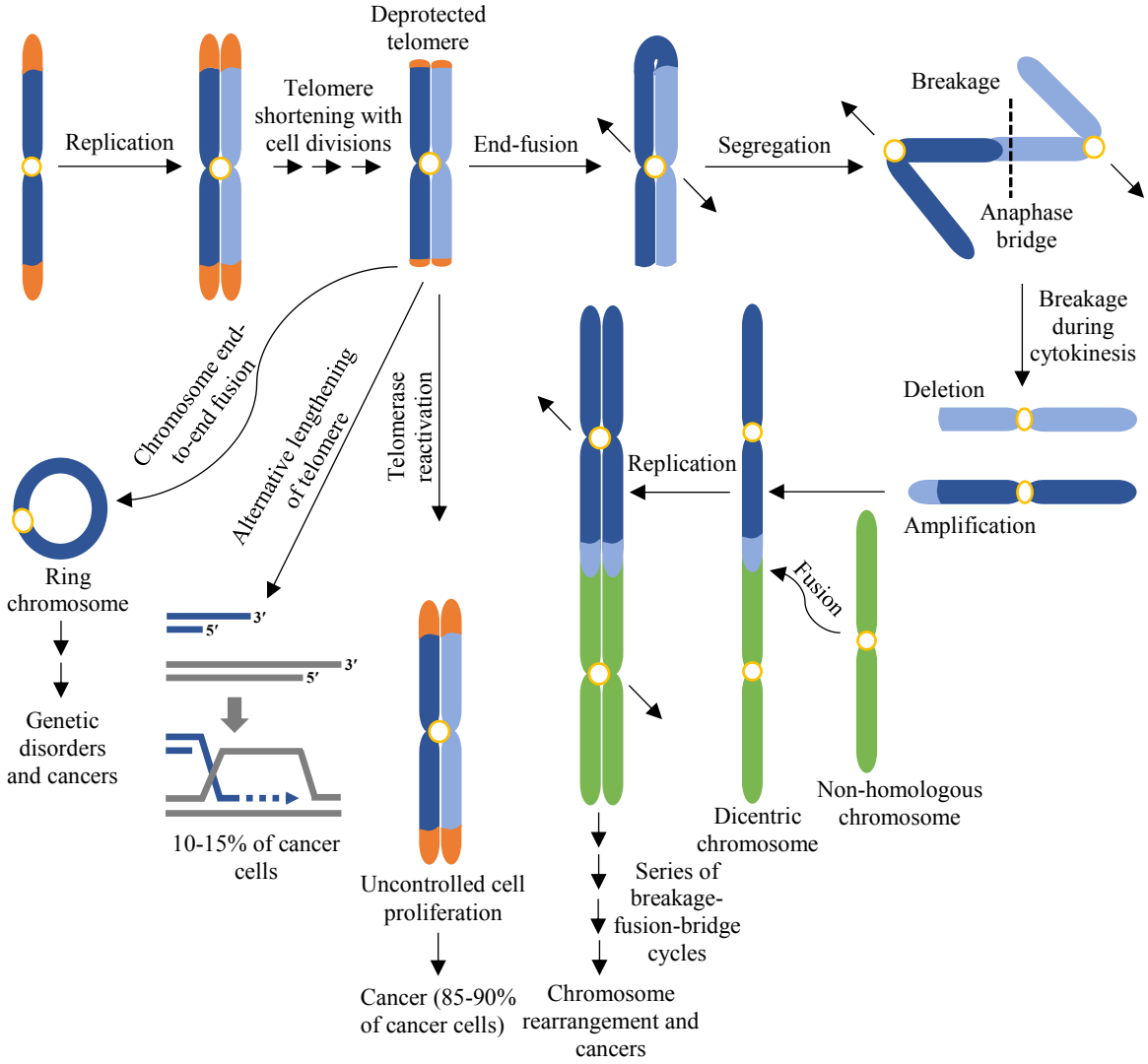

Fig. 1.5. Telomere dysfunction and genome instability in cancers. Telomere deprotection as a consequence of telomere shortening with cell divisions induces chromosome end fusions and formation of dicentric chromosomes which trigger series of breakage-fusion-bridge cycles that lead to genomic rearrangement and cancers. Cells can escape telomere shortening through reactivation of telomerase or maintain telomere length by recombination in a mechanism known as alternative lengthening of telomeres (ALT), producing potential tumorigenic cells. Intrachromosomal end-to-end fusion followed telomere dysfunction can produce ring chromosomes which lead to genetic disorders and cancers.

1.2 RecQ helicase and recombination-dependent telomere maintenance

RecQ protein family is highly evolutionarily conserved DNA helicases that play important roles in numerous processes of DNA metabolism such as DNA replication, recombination, repair, and transcription [43]. RecQ helicases play important roles in replication, recombination, and repair at telomeres and recruited to telomeres in a cell cycle-dependent manner [43]. In mammals, RecQ helicase consists of five members RECQL1, BLM, WRN, RECQL4, and RECQL5 [43]. In yeast, there is only one RecQ helicase member has been identified as Rqh1 (the homolog of human BLM in *S. pombe*) [44] and Sgs1 (the homolog of human BLM in *S. cerevisiae*) [45]. Dysfunction of human RecQ helicases results in genetic diseases, aging, and cancer which are mostly linked to telomere shortening. [46].

In *S. cerevisiae*, Sgs1 helicase plays a role in the maintenance of telomeres through recombination in the absence of telomerase [47]. Similarly, human BLM helicase can maintain telomeres in ALT cells [48]. Both BLM and WRN bind to telomeric DNA during S-phase in ALT cells, and the overexpression of BLM can lengthen the telomeres in these cells [48, 49], indicating that BLM and WRN have an important role in the maintenance of telomeric integrity in the absence of telomerase.

1.2.1 Functional interaction between Pot1 and RecQ helicases

Although fission yeast *pot1*Δ *rqh1*Δ double mutant is synthetically lethal [50], the double mutation between *pot1*Δ and *rqh1-hd* (helicase-dead point mutation) is alive and can maintain telomeres through HR (Fig. 1.6A), a phenotype reminiscent of human ALT cancer cells [51]. One possible explanation is that the helicase activity of Rqh1 may be involved in the resection of telomeres in the absence of Pot1. Second, the helicase activity of Rqh1 may be important to suppress the aberrant accumulation of recombination intermediates at telomeres. Intriguingly, the *pot1*Δ *rqh1-hd* double

mutant is sensitive to microtubule inhibitor TBZ (Fig. 1.6B). A possible explanation for this TBZ sensitivity phenotype is that the recombination intermediates at telomeres exist till M-phase resulting in a physical link between sister chromatids making it difficult to separate them upon inhibition of microtubules by TBZ which eventually results in cell death. Interestingly, the dual inhibition of human POT1 and RecQ helicase WRN results in sensitivity to microtubule inhibitor drug (vinblastine), indicating that the functional interaction between fission yeast Pot1 and Rqh1 and human POT1 and WRN is conserved [51] and implying that inhibition of WRN in ALT cells would enhance the sensitivity of ALT cells to microtubule inhibitors. Consequently, fission yeast *pot1*Δ *rqh1-hd* double mutant would help understand the behavior of cells that maintain telomeres by HR which would be of clinical outcomes in the treatment of ALT cancer cells.

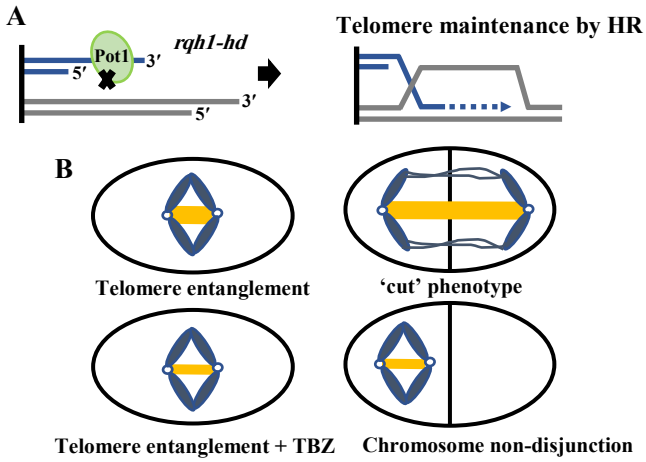

Fig. 1.6 (A) A schematic representation of the telomere maintenance by homologous recombination in the *pot1*Δ *rqh1-hd* double mutant. The recombination intermediates accumulate at the chromosome ends of the double mutant. (B) Model of chromosome segregation defects in the *pot1*Δ *rqh1-hd* double mutant. A pair of sister chromatids of the *pot1* Δ *rqh1-hd* double mutant with entangled chromosome ends during M-phase. The small circle represents centromere/kinetochore. The thick line represents the normal mitotic spindle while the thin line represents the destabilized spindle in the presence of TBZ. Fig. 1.6B captured from the work of Takahashi K. et al. Mol. Cell. Biol. 31: 495– 506 (2011).

1.3 Circular chromosomes (Ring chromosomes)

Circular chromosomes are also known as ring chromosomes (RCs), a term that had been first proposed by Cote *et al.* [52]. RCs are a rare cytogenetic anomaly that has been reported in all human chromosomes. RCs are circular DNA molecules that can be formed because of breakage at both arms of chromosomes generating sticky ends ready for fusion with loss of some genetic materials at the broken regions [2, 53]. Alternatively, RCs can be formed due to telomere dysfunction through fusion between subtelomeric sequences, telomere-telomere or telomeric-subtelomeric fusion without loss of genetic materials generating complete ring chromosome [53, 54]. Nevertheless, individuals with complete ring may have a deletion on microscopic levels that cannot be detected using standard cytogenetic techniques. RCs can also be classified into two main types with different clinical phenotypes; the non-supernumerary ring in which RC replaces one of the normal chromosomes resulting in a 46, (r) karyotype and the supernumerary ring in which the individual carries extremely small extra chromosome in addition to the normal 46 chromosomes with 47, +(r) karyotype [53, 55]. RCs have also been described in other eukaryotes such as *Drosophila,* maize (*Zea mays*) and fission yeast [30, 31, 56, 57].

How cell with RCs normally segregates its circular chromosomes and passes through mitosis depends on whether the RCs undergo sister chromatid exchanges (SCEs) before cell division or not [55]. If no SCEs occur at the breakpoint, cells with RCs can normally proceed through mitosis, and the separation of ring chromatids would normally occur without problem producing two equal-sized rings with a centromere each (Fig. 1.7A). In the case of an odd number of SCEs, rings will double in size producing a dicentric double-sized ring with two centromeres. The anaphase segregation of dicentric ring can lead to chromosome breakage and formation of

anaphase bridge. This chromosome breakage can result in more genetic instability including loss or amplification of genetic materials, a reunion of different broken fragments, or ring loss in subsequent cell divisions (Fig. 1.7B). If an even number of SCEs occur, RCs can either segregate without problem or can form interlocked rings, which upon chromosome segregation can produce a ring or chromosome breakage (Fig. 1.7C).

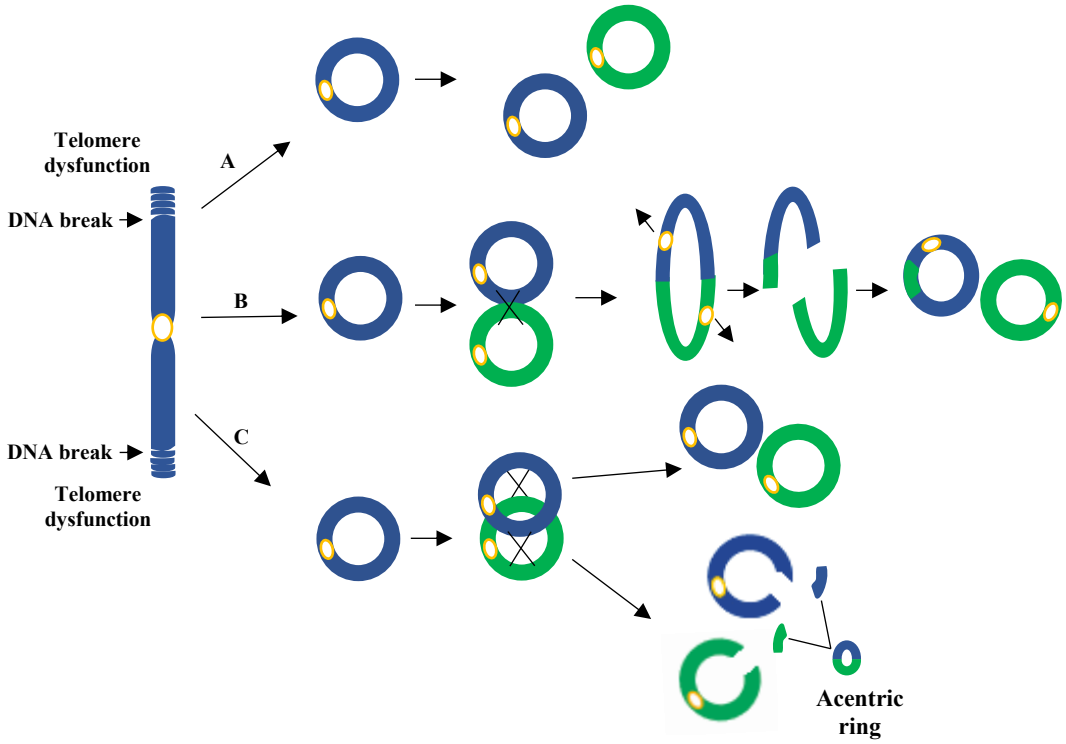

Fig. 1.7. RC instability during the cell cycle. (A) Rings undergo no SCEs and normally proceed through mitosis producing two rings. (B) RC undergoes an odd number of SCEs resulting in the dicentric double-sized ring with two centromeres. During chromosome segregation, the ring either breaks and forms a new ring with further deletion or duplication of genetic materials or the entire dicentric ring passes into one daughter cells, producing monosomic cells. (C) RC undergoes even number of SCEs. The two rings can either normally segregate producing two normal rings or form interlocked rings that break in the subsequent cell divisions. Inspired by the work of Inna E. Pristyazhnyuk and Aleksei G. Menzorov; doi: 10.1007/s00709-017-1165-1 with slight modifications.

1.3.1 Ring chromosomes: genetic disorders and cancers

RCs are structurally unstable and cells with rings can undergo series of chromosome instability (CIN) during cell divisions such as chromosome nondisjunction, anaphase bridge, ring fragmentation, nuclear projection, micronuclei, pulverized chromosomes which can eventually lead to the production of secondary aneuploid cells with possible deleterious consequences, in particular, cancers [58-59]. Continuous production of secondary aneuploid cells can contribute to tumorigenesis and developmental disorders such as decreased weight at birth, mental retardation, and growth retardation, the major physical abnormality of the ring syndrome [58, 60]. Even though the ring syndrome is not specific and can interfere with symptoms of different pathological origins, some patients with RCs have unique symptoms such as refractory epilepsy that associates with RC20 [61].

In addition to the association of RCs with some genetic disorders, RCs have been reported in a wide variety of human neoplasia [62]. For instance, dermatofibrosarcoma protuberans (70%), acute myelogenous leukemia, atypical lipomatous tumors (63%), acute lymphoblastic leukemia (3.4%), malignant mesenchymoma, parosteal osteosarcoma, pancreatic carcinoma (more than 10%), hematopoietic malignancies (less than 10%), urinary bladder tumors (more than 15%), low-grade malignant fibrous histiocytoma (MFH), mesenchymal tumors (more than 70%) and some others [62]. The highest incidence of RCs occurred in mesenchymal tumors. However, RCs are very rare in some tumors such as epithelial tumors, nervous system, breast and ovarian cancers [62].

Till now, the mechanism behind the formation of RCs in human neoplasia and how cells with RCs could survive are largely enigmatic. One possibility is that the RCs can lead to tumor development if the tumor suppressor genes loci are affected by the

ring formation [63]. Alternatively, chromosomal alteration such as amplification of the genes that negatively regulate tumor suppressor genes can also lead to cancers [64].

1.3.2 Clinical management of ring chromosomes

To date, no possible therapeutic strategies for treatment of RCs disorders have been described. Most of the treatment prescribed so far are symptomatic and supportive. For example, antiepileptic drugs are the main treatment strategy to control the epileptic attacks in patients with RC20 [61]. Surgery intervention remains a preferred option to repair malformations associated with RCs and for tumor excision. Drug treatment using a tyrosine kinase inhibitor, imatinib, had also been described for the treatment of recurrent or metastatic dermatofibrosarcoma protuberans [65]. Recently, some studies point out toward "chromosome therapy" strategy as a therapeutic intervention for correction of RCs [66, 67].

In conclusion, treatment of ring chromosome-associated diseases still represents a clinical dilemma. Further understanding about the mechanisms of survival of cells with RCs is needed to help develop a strategy for selective targeting of pathogenic cells with RCs.

1.4 Fission yeast *Schizosaccharomyces pombe* as a model organism

Although both fission yeast and budding yeast are ascomycetes, fission yeast is approximately 1000 million years evolutionary distant from budding yeast [68, 69]. Fission yeast, commonly known as *Schizosaccharomyces pombe*, was originally isolated by German scientist Paul Lindner in 1893 from East African millet beer [70]. Lindner named it *Schizosaccharomyces pombe* in which "*Schizo*" refers to the cells divide by fission to differentiate it from budding yeasts that divide by bud formation and "*pombe*" is the Swahili word for beer since it was originally isolated from East African millet beer [70]. Fission yeast had been developed as an experimental model in

the early 1950s by Swiss geneticist Urs Leupold who isolated two homothallic strains (968 h^{90} and h^{40}) and two heterothallic strains of opposite mating type (975 h^{+} and 972 h^{-}) [71, 72]. Three of these isolates 968 h^{90}, 975 h^{+}, 972 h^{-} had primed and established the infrastructure of yeast genetics and commonly used in nearly all laboratory using fission yeast as model organism nowadays.

S. pombe is a rod-shaped unicellular simple eukaryote with 7-14 μm in length and 3-4 μm wide that grows in length by tip elongation until reaching certain cell size before initiation of cell division and divides by medial division (Fig. 1.8A). This mode of cell growth by increasing length is used as an indicator for the stage of the cell cycle at which the longest cells are those about to commit mitosis, and the shortest ones are those that are newly born after the completion of cytokinesis [73]. Yeast cells are predominately existing in a haploid state (contains one set of chromosomes) which is useful to screen for mutants that produce a specific phenotype. Diploid state (contains two sets of chromosomes) can also be maintained and can be used to determine whether a mutant allele is dominant or recessive relative to the wild-type. Diploid cells are much larger in length and width than haploid. Yeast cells are easy to be genetically manipulated because they possess efficient HR mechanisms which allow for ease introduction of novel genetic materials [74]. Furthermore, fission yeast can be easily maintained and grown in the lab using an inexpensive wide range of media and has quite a fast cell cycle with cell doubling time about 2-4 h for the wild-type depending on the medium and the temperature [75].

Meiosis in fission yeast occurs by mating heterothallic haploid cells with opposite mating type h^{+} and h^{-} or as a self-cross of homothallic strain (h^{90}), which possesses the information of both mating types, under a condition of nitrogen starvation which typically arrests cells in G1 [76]. Upon conjugation, the nuclei of mating cells

fuse to form diploid zygotic ascus characterized by zig-zag or banana-like shape which precede to meiosis, if the starvation condition persists, producing four haploid ascospores that can enter vegetative mitotic cell cycle once the conditions become favorable (Fig. 1.8B).

Fission yeast undergoes a typical eukaryotic cell cycle divided into G1 (gap 1), S (synthesis), G2 (gap 2), and M (mitosis) phases. G1, S, and G2 are collectively known as "interphase". The fission yeast cells spend most of their time in G2 (about 70%), and the remaining 30% is divided equally among G1, G2, and S-phases (Fig. 1.8B) [75]. Cells can undergo mitosis with intact nuclear envelope, a process called "closed mitosis" [77]. Since the G1 phase is very short in fission yeast, the cells start DNA replication very soon after mitotic exit, and the completion of cytokinesis occurs at S-phase. Therefore, the newly born daughter cells are almost in G2 phase [75].

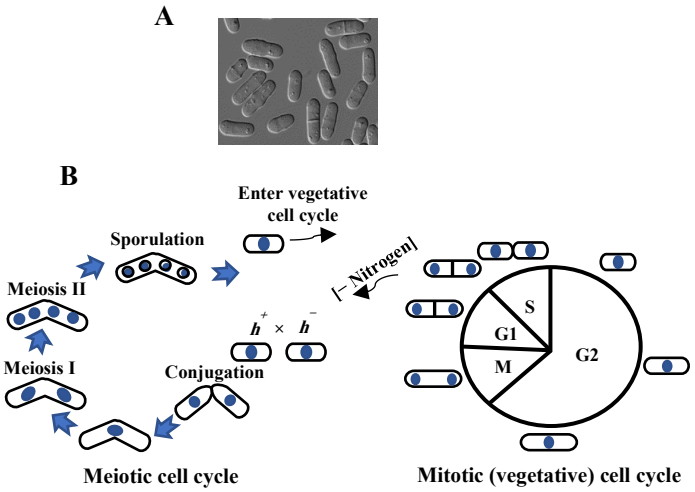

Fig. 1.8. (A) Representative pictures of vegetative growing wild-type (*WT*) *S. pombe* cells. (B) Schematic representation of fission yeast life cell cycle. On the right, the mitotic cycle showing the main four phases G2, M, G1, and S-phase. On the left, the meiotic cycle is triggered in response to starvation (e.g. nitrogen starvation) by mating the two haploid strains of opposite mating type. Upon conjugation, the nuclei of mating cells fuse to form diploid zygotic ascus characterized by zig-zag or banana-like shape which precede to meiosis producing four haploid ascospores that can enter vegetative mitotic cell cycle once the conditions become favorable. Picture of Fig. 1.8B is inspired by the Forsburg lab *pombe* page; http://www-bcf.usc.edu/~forsburg/main4.html.

Fission yeast is the sixth eukaryotic organism whose entire genome was sequenced following *Saccharomyces cerevisiae*, *Caenorhabditis elegans*, *Drosophila melanogaster*, *Arabidopsis thaliana* and *Homo sapiens* [78-83]. The complete genome sequence was published in 2002 showed that fission yeast haploid cell has a small and compact genome of 13.8 Mb in size, compared to the 12.5 Mb of *Cerevisiae* genome, divided between three chromosomes; Chr. I (5.7 Mb), Chr. II (4.6 Mb) and Chr. III (3.5 Mb) [83]. This small genome provides an advantage for easier genetic manipulation compared with the budding yeast that harbors 16 chromosomes. *S. pombe* cell has 5059 protein-coding genes with 67% of the genes are closely similar to that of human disease-related genes [83], providing it as a powerful tool to study various biological processes which are conserved from yeast to human.

The genome organization patterns in fission yeast share a number of features with those of metazoans: the telomere, centromere, and origin of replication are much like higher eukaryotes compared with budding yeast [83]. Fission yeast provides a powerful tool for studying many biological processes such as the RNAi pathway, centromere functions, DNA replication, checkpoint, and cell cycle studies, and telomeres compared with budding yeast.

In fission yeast, the telomeres at chromosomes I and II contain a repetitive sequence of 20-40 kb known as subtelomeric elements (STE1), (STE2), and (STE3) that extend from telomere toward centromere. On chromosome III, the subtelomeric regions were replaced with rDNA repeats at both chromosome arms [9]. The telomere proteins that cap the end of fission yeast chromosomes show a striking similarity to those of mammals compared with budding yeast. Moreover, the low number of chromosomes in fission yeast compared with budding yeast allows for ease genetic manipulation and production of specific phenotypes such as chromosome

circularization. The chance for all chromosomes to be circularized is inversely proportional to the number of chromosomes cells have. In fission yeast, circularization of all three chromosomes has been reported in some mutants, while it was not observed in budding yeast, providing an advantage for the use of fission yeast to study the behavior of ring chromosomes and the molecular mechanisms of their maintenance.

1.5 The aim of the thesis

Telomere dysfunction is one of the key driving forces for genomic instability and cancers. For instance, recombination-dependent telomere maintenance and chromosome circularization following telomere dysfunction had been reported in association with cancers. My thesis aims to identify vulnerable points in these two telomere dysfunction cases which would help find a possible target for cancer therapy. To this end, I performed the following two studies:

1. Understand the reason behind the TBZ sensitivity phenotype of the *pot1*Δ *rqh1-hd* double mutant.

The fission yeast *pot1*Δ *rqh1-hd* double mutant maintains telomere by HR, a phenotype resembles cancer cells that maintain telomere by recombination, and sensitive to anti-microtubule TBZ [51]. However, the mechanism of the TBZ sensitivity phenotype of the *pot1*Δ *rqh1-hd* double mutant is not well understood. Identifying the mechanism of the TBZ sensitivity of the *pot1*Δ *rqh1-hd* double mutant would enable me to find a specific vulnerability in cancer cells that maintain telomeres by recombination which could be a target to sensitize these cancer cells to anti-microtubule drugs. Therefore, I tried to understand the reason behind the TBZ sensitivity phenotype of the *pot1*Δ *rqh1-hd* double mutant.

2. Define a gene required for the maintenance of a circular chromosome and the survival of cells having circular chromosomes.

Chromosome circularization has been observed in association with human cancers [62]. Till now, the mechanisms behind the maintenance of circular chromosomes and how cells with circular chromosomes could survive are largely enigmatic. Using fission yeast *pot1*Δ cells that have circular chromosomes, I attempted to define a gene required for the survival of cells having circular chromosomes. This gene could be a target of cancer therapy to selectively kill cancer cells that harbor circular chromosomes.

Chapter 2. Long G2 accumulates recombination intermediates and disturbs chromosome segregation at dysfunction telomere in *Schizosaccharomyces pombe*

Note: This study was published in Biochemical and Biophysical Research Communications [84]. Most of the figures and tables in this chapter were reproduced from the published article with slight modifications.

2.1 Introduction

Cell cycle checkpoints are a surveillance mechanism that tightly regulates cell cycle progression [85]. In the presence of DNA damage, checkpoints impede the cell cycle progression to provide cells with time to repair the damaged DNA, thus ensuring faithful transmission of the genome [86]. Failure to enforce DNA damage checkpoint in the presence of DNA damage can lead to genome instability and cancers [86, 87].

In fission yeast, Chk1 is an effector kinase that mediates the DNA damage checkpoint signaling [88]. Chk1 is required for the DNA damage checkpoint response but not the replication checkpoint and functions under the regulation of a group of checkpoints "Rad proteins" that include Rad1, Rad3, Rad9, Rad17, Rad26, and Hus1 [89, 90]. In response to the DNA damage, Rad3 phosphorylates the downstream kinase Chk1 resulting in Chk1 activation [91]. Active Chk1 phosphorylates the downstream kinases Wee1 and Mik1 which in turn phosphorylate Cdc2 at the highly conserved tyrosine-15 (Y15) residue, keeping it in an inactive state and hold the cells at the G2/M boundary [92, 93]. Cdc2, together with its regulatory subunit cyclin B, is the key regulator that orchestrates the transition through the cell cycle phases [94, 95]. The activation of Cdc2-cyclin B complex

through its de-phosphorylation at Y15 with Cdc25 phosphatase is the rate-limiting step that triggers the G2/M transition and mitotic entry [96]. Therefore, the loss-of-function of Wee1 and Mik1 or the overexpression of Cdc25 can override the cell cycle checkpoint and elicit a premature mitotic entry at a smaller size than that of the wild type [93, 94].

The telomeres in *pot1*Δ *rqh1* helicase dead *(rqh1-hd)* point mutant, in which lysine 547 is mutated to alanine are maintained by HR in a Rad51-dependent manner [51]. The recombination intermediates accumulate at the chromosome ends of the *pot1*Δ *rqh1-hd* double mutant and exist till mitosis resulting in disturbance of chromosome segregation and render cells sensitive to TBZ [51]. The *pot1*Δ *rqh1-hd* double mutant cells display long G2 phenotype, implying the activation of the DNA damage checkpoint. Interestingly, deletion of $chk1^{+}$ or mutation of its kinase domain, in which aspartic acid 155 is mutated to alanine which has no kinase activity in vitro, shortened the G2 of the *pot1*Δ *rqh1-hd* double mutant and suppressed the accumulation of the telomeric recombination and the TBZ sensitivity [97]. A notion emerged from these results is whether there is a link between the long G2 of the *pot1*Δ *rqh1-hd* double mutant and its TBZ sensitivity.

In this study, I found that shortening the G2 of the *pot1*Δ *rqh1-hd* double mutant suppressed the TBZ sensitivity and the accumulation of recombination intermediates at the telomeres of *pot1*Δ *rqh1-hd* cells. My results imply that the long G2 is the cause of the TBZ sensitivity of the *pot1*Δ *rqh1-hd* double mutant in the way that long G2 provides *pot1*Δ *rqh1-hd* cells with time for the accumulation of recombination intermediates at the chromosome ends which disturb chromosome segregation and render cells sensitive to TBZ.

Table 2.1 *Schizosaccharomyces pombe* strains used in this study

Strain	Genotype	Source
GT000	*h^+ leu1-32 ura4-D18 ade6-M210 pot1::kanMX6 rqh1-K547A (pPC27-ura4-pot1$^+$-HA)*	Takahashi et al.
GT002	*h^- leu1-32 ura4-D18 ade6-M210 pot1::kanMX6 rqh1-K547A*	Takahashi et al.
FY16194	*h^- ade6-M216 ura4-D18 cdc2-3w*	NBRP
AH010	*h^- leu1-32 ura4-D18 ade6-M210 pot1::kanMX6 rqh1-K547A cdc2-3w (pPC27-ura4- pot1$^+$-HA)*	This study
AH009	*h^- leu1-32 ura4-D18 ade6-M210 pot1::kanMX6 rqh1-K547A cdc2-3w*	This study
MY444	*h^- leu1-32 ura4-D18 wee1-50 mik1::ura4$^+$*	NBRP
KM032	*h^+ leu1-32 ura4-D18 pot1::kanMX6 rqh1-K547A wee1-50 mik1::ura4$^+$ (pPC27-leu1- pot1$^+$-HA)*	This study
KM031	*h^+ leu1-32 ura4-D18 pot1::kanMX6 rqh1-K547A wee1-50 mik1::ura4$^+$*	This study
TH025	*h^+ leu1-32 ura4-D18 ade6-M210 pot1::kanMX6 rqh1-K547A (pPC27-leu1- pot1$^+$-HA)*	Nakano et al.
YI002	*h^- leu1-32 ura4-D18 ade6 pot1::kanMX6 (pPC27-ura4-pot1$^+$-HA)*	Nanbu et al.
SIH60	*h^- leu1-32 ura4-D18 ade6 pot1::kanMX6 rav1::hphMX6*	This study

2.2 Materials and methods

2.2.1 Mating (Random spore analysis)

Mix a loopful of freshly growing h^+ and freshly growing h^- cells in an Eppendorf tube containing 10 μL sterile water. Spread the cells on malt extract (ME) (3% Bacto™ malt extract) media to an area of 1 cm^2. Leave the cross to dry and incubate at 25ºC to 2-3 days. Examine under the light microscope for the formation of four spore zygotic asci. Pick a loopful of mated cells from the mating plate into an Eppendorf tube containing 100 μL sterile water, then add 10 μL 0.5% glusulase and incubate overnight at 25ºC. Using hemocytometer, confirm there are no complete asci exist. Wash off the spores from the glusulase by centrifugation and re-suspend the cells in 100 μL sterile water. Plate the cells

into suitable media and incubate till the formation of colonies (it takes 3-5 days depending on the temperature).

2.2.2 Strain construction

The *pot1*Δ *rqh1-hd wee1-50 mik1*Δ mutant cells (*pot1::kanMX6 rqh1- K547A wee1-50 mik1::ura4*$^+$) expressing Pot1 from plasmid (pPC27- pot1$^+$-hemagglutinin [HA], containing *leu1*$^+$) were constructed by mating *h*$^+$ *pot1*Δ *rqh1-hd* double mutant (*pot1::kanMX6 rqh1-K547A* (pPC27-leu1-pot1$^+$-HA) with *h*$^-$ *wee1-50 mik1::ura4*$^+$ double mutant. Cells were streaked on Edinburgh minimal medium (EMM) (1% glucose, 0.5% NH_4Cl, 0.45% $Na_2HPO_4.\ 12H_2O$, 4% salt solution, 1% vitamin solution, 1% trace element) lacking uracil to select for *mik1::ura4*$^+$ mutation and on yeast extract agar (YEA) (0.5% Bacto^{TM} yeast extract, 3% glucose, and 40 µg/mL adenine) plates containing G418 disulfide (100 µg/mL) at 25ºC to select for *pot1::kanMX6* mutation. Candidate cells were re-streaked on YEA plates containing 4 mM Hydroxyurea (HU) at 25ºC to select cells harboring *rqh1-hd* mutation (cells that cannot grow in the presence of HU are cells with *rqh1-hd* mutation). Candidates were re-streaked on YEA at 36ºC to select for *wee1-50* mutation. The *pot1*Δ *rqh1-hd wee1-50 mik1*Δ mutant cells that do not have pPC27-*pot1*$^+$-HA were selected on YEA plates containing 100 µM 5-fluorodeoxyuridine (FUDR).

The *pot1*Δ *rqh1-hd cdc2-3w* triple mutant (*pot1::kanMX6 rqh1-K547A cdc2-3w*) expressing Pot1 from a plasmid (pPC27-*pot1*$^+$ [HA] , containing *ura4*$^+$) was constructed by mating *h*$^+$ *pot1*Δ *rqh1-hd* double mutant (*pot1::kanMX6 rqh1-K547A)* expressing Pot1 from a plasmid (pPC27-*pot1*$^+$ [HA], containing *ura4*$^+$) with *h*$^-$ *cdc2-3w*. Cells were streaked on YEA plates containing G418 disulfide at 25ºC to select for *pot1::kanMX6* mutation and on YEA plates containing 4 mM HU to select for *rqh1-hd* mutation. Since

cdc2-3w cells characterized by small-sized cells with short G2, the *pot1*Δ *rqh1-hd* cells with small size were selected as the *pot1*Δ *rqh1-hd* cells carrying the *cdc2-3w* mutation. The *pot1*Δ *rqh1-hd cdc2-3w* triple mutants that do not have the Pot1 plasmid were counter-selected on YEA plates containing 2 g/L 5-fluoroorotic acid (FOA).

2.2.3 Measurement of telomere length

Telomere length was measured using Southern hybridization. Ten mL of exponentially growing log-phase cells are harvested by centrifugation at 5000 rpm for 10 min at room temperature. Discard the supernatant and re-suspend the cell pellets in 100 µL lysis buffer (2% Triton X, 1% SDS, 10 mM Tris-HCl [pH 8.0], 10 mM EDTA, 5 mM NaCl) and transfer to 1.5 mL Eppendorf tube. Add ~100 µL volume of acid-washed glass beads and 100 µL of phenol/chloroform and vortex at high speed for 30 min at 4^{o}C. Spin down the tube at high speed and add 100 µL lysis buffer and 100 µL phenol/chloroform. Vortex, spin down and add 200 µL TE buffer (10 mM Tris-HCl [pH 8.0], 1 mM EDTA). Vortex the mixture and centrifuge at 15000 rpm for 10 min at room temperature. Transfer the aqueous layer (top layer) ~400 µL to new Eppendorf tube containing 100 µL phenol/chloroform and centrifuge one more time at 15000 rpm for 10 min at room temperature. Transfer the aqueous layer into a new Eppendorf tube, add 400 µL 2-propanol and 40 µL 3 M sodium acetate [pH 5.2], mix, and wait for ~10 min. Centrifuge at 15000 rpm for 10 min at room temperature (the DNA will precipitate at this stage). Wash the DNA pellets with ~500 µL 70% ethanol and centrifuge at 15000 rpm for 5 min at room temperature. Pour off the ethanol, dry up the DNA and re-suspend the DNA pellets in 100 µL TE buffer. Then 1 µL of 1 µg/mL RNase solution is added to degrade the RNA. Incubate at 37^{o}C for 4 h and then confirm the degradation of RNA by gel electrophoresis.

To extract the DNA after the RNA digestion, add 100 µL phenol/chloroform and centrifuge at 15000 rpm for 10 min at room temperature. Transfer the upper layer containing the DNA into a new tube and add 2.5× 100% ethanol and 0.1× 3 M sodium acetate and keep at -20 for ~30 min to allow the precipitation of DNA. Centrifuge at 15000 rpm for 10 min at 4°C. Wash the precipitated DNA pellets with 500 µL 70% ethanol and centrifuge at 15000 rpm for 5 min at 4°C. Pour off the ethanol and dry up the DNA. The genomic DNA was then digested with EcoRI and separated on 1.5% agarose gel. The separated DNA is then transferred to a positively charged nylon membrane by the process of blotting. During the aspiration, gel was mounted with denaturation buffer (1.5 M NaCl, 0.5 N NaOH) for 12 min, aspirated and mounted with neutralization buffer (1 M Tris-HCl [pH 5.0], 2 M NaCl) for 12 min, then aspirated and mounted with 20X SSC (3 M NaCl, 0.3 M trisodium citrated dehydrate) for 1 h. The membrane was then cross-linked by UV cross-linker (1200 J/m^3) and probed with DNA fragment containing telomere and telomeric-associated sequence 1 (TAS1) derived from pSNU70, which was amplified by PCR using pITNI as a template and purified with Gel Extraction Kit (QIAGEN). Hybridization with the probe was done according to the manufacture protocol (AlkPhos Direct™, GE Healthcare). The single-stranded telomeric DNA probe was labeled with (γ-^{32}P ATP) (GE Healthcare) by using T4 polynucleotide kinase. The membrane was placed in 50 mL tube (membrane is oriented with DNA side facing the interior of the tube) and hybridized overnight with hybridization buffer (Rapid-Hyb Buffer; GE Healthcare) and the ten pmol probe at 55°C. Discard the hybridization buffer but keep the membrane inside the tube and wash the membrane twice with 100 mL primary wash buffer at 55°C for 10 min. Pour off the primary wash buffer, remove the membrane from the tube and place it in a small plastic box with lid, with the

DNA side up, and wash the membrane twice with gentle agitation with 100 mL secondary wash buffer for 5 min at room temperature. Pour off the excess secondary wash buffer and add ~700 µL CDP-Star^{TM} detection reagent onto the membrane surface and let sit for 5 min. Drain off the excess detection reagent, wrap the membrane and detect the chemiluminescent signal using FujiFilm LAS-3000 mini imaging system.

2.2.4 Pulsed-field gel electrophoresis (PFGE)

Fifty mL of exponentially growing log-phase cells were collected by centrifugation at 5000 rpm for 3 min. Re-suspend the cell pellets with SPI buffer (1.2 M sorbitol, 50 mM sodium citrate, 30 mM Na_2HPO_4. $12H_2O$, 40 mM EDTA pH [5.6]) to reach a cell density of 5.5×10^8 cells/mL. For each five agarose plugs, 10^8 cells were treated with Zymolyase-100^T (2 mg/mL) for 2 h at 37ºC. Cells were collected by centrifugation at 5000 rpm for 3 min and re-suspended in 25 µL TSE buffer (10 mM Tris HCl [pH 7.5], 0.9 M sorbitol, 45 mM EDTA). Low-melt preparative grade agarose (Bio-Rad, Richmond, CA) was added from a 1% solution in TSE buffer equilibrated at 43ºC, and the cell suspension was transferred into four plug molds. Solidified plugs were washed in PW1 (50 mM Tris-HCl [pH 7.5], 0.25 M EDTA, 1% SDS) for 2 h at 50ºC, transferred into PW2 (10 mM Tris-HCl [pH 9.0], 0.25 M EDTA, 1% w/v N-lauroylsarcosine, 1 mg/mL proteinase K) and incubated for 24 h at 50ºC. Plugs were incubated at 50ºC in fresh PW2 for another 24 h, washed extensively twice in 10 mL T10×E (10 mM Tris-HCl [pH 7.5], 10 mM EDTA), and incubated at 4ºC for 30 min. Treat the plugs twice with 10 mL T10×E and 23 µL phenylmethylsulfonyl fluoride (PMSF) and incubate at 50ºC for 30 min. Wash the plugs twice with 10 mL T10×E and incubate at room temperature for 30 min. Wash the plugs twice with 1 mL sterile TE buffer and incubate at 4ºC for 16 min. Transfer the plugs to 50

mL Falcon tube containing 10 mL 3 buffer (NEB), 100 µL Bovine serum albumin (BSA) (10 µg/mL) and 100 µL Dithiothreitol (DTT) (100 mM) and incubated overnight at 37ºC. Transfer the plugs into new Eppendorf tube containing 300 µL 3 buffer, 3 µL BSA, 3 µL DTT and restriction enzyme NotI (40 unit) and incubate at 37ºC for 2 h. Add another 40 unit of NotI and incubate overnight at 37ºC. Wash the plugs with 1.5 mL T10×E buffer and incubate at 4ºC for 30 min. Transfer the plugs to new Eppendorf tube containing 1 mL 0.5×TBE buffer (50 mM Tris-HCl, 5 mM boric acid, 1 mM EDTA, [pH 8.0] and incubate at 4ºC for 30 min. The NotI-digested chromosomal DNA was then fractionated in 1% agarose gel with 0.5% sterile TBE buffer at 14ºC using the CHEF Mapper PFGE system at 6 v/cm (200 V) and a pulse time of 60-120s over 24 h. The DNA was visualized by staining the gel with ethidium bromide (EtBr) (200 mL 0.5×TBE + 200 µL EtBr). The DNA was then blotted onto Hybond-N+ nylon membrane, and the procedures were then continued as same as Southern hybridization using probes that were amplified from pITNI by PCR and purified with Gel Extraction Kit to M, L, I, C probes.

2.2.5 Microscopy

Microscope images of living cells were obtained using an AxioCam digital camera (Zeiss) connected to an Axio Observer. Z1 microscope (Zeiss) with a Plan-Apochromat 63× objective lens (numerical aperture, 1.4). Pictures were captured and analyzed using AxioVision Rel. 4.8.2 software (Zeiss).

2.3 Results

2.3.1 Concomitant loss-of-function of *wee1*$^+$ and *mik1*$^+$ suppressed the TBZ sensitivity of the *pot1*Δ *rqh1-hd* double mutant

The fission yeast cells spend most of their time in G2. The activation of Chk1 in response to DNA damage and the subsequent activation of its downstream kinases Wee1 and Mik1 impede cell cycle progression and hold the cells at the G2/M boundary with long G2 till the repair of the damaged DNA [88-93]. Interestingly, the long G2 of the *pot1*Δ *rqh1-hd* double mutant was suppressed by deletion of *chk1*$^+$ or mutation of its kinase domain, implying the activation of the DNA damage checkpoint in that double mutant (Fig. 2.1). Moreover, deletion of *chk1*$^+$ or mutation of its kinase domain suppressed the TBZ sensitivity of *pot1*Δ *rqh1-hd* cells (Fig. 2.2A), suggesting a possible link between the long G2 phenotype of the *pot1*Δ *rqh1-hd* double mutant and its TBZ sensitivity. If this is the case, then I might expect that the loss-of-function of Chk1 downstream kinases, Wee1 and Mik1, would also shorten the G2 of the *pot1*Δ *rqh1-hd* double mutant and alleviate its TBZ sensitivity. Wee1 delays the onset of mitotic entry in response to DNA damage and to allow time for the cells to attain a suitable size before mitotic entry. The concomitant loss-of-function mutation of *wee1*, *wee1-50* which is a temperature-sensitive mutant allele of *wee1*, and the null mutation of the *mik1*$^+$ trigger a premature mitotic entry at a decreased cell size compared with the wild-type [93]. Indeed, *wee1-50 mik1*Δ double mutation shortens the G2 of the *pot1*Δ *rqh1-hd* double mutant (Fig. 2.1).

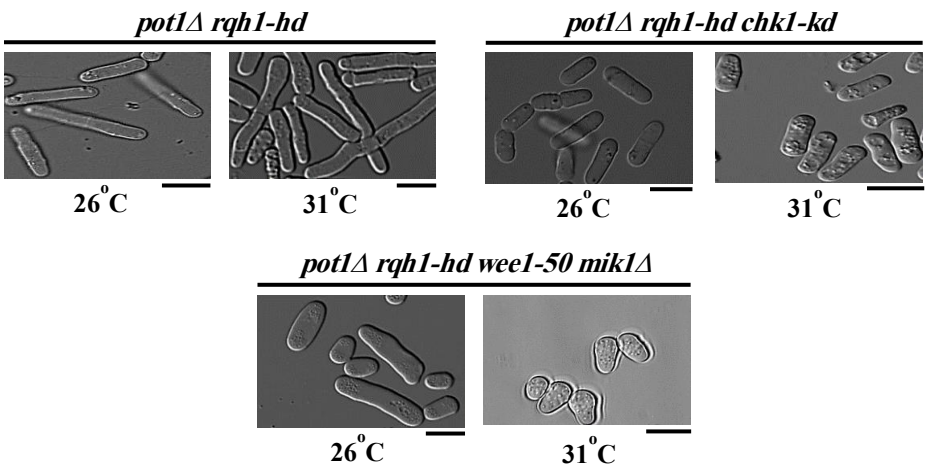

Fig. 2.1. The cell length of vegetative growing *pot1*Δ *rqh1-hd* cells, *pot1*Δ *rqh1-hd chk1-kd* cells and *pot1*Δ *rqh1-hd wee1-50 mik1*Δ cells at the indicated temperatures. Bar =10 μm.

To investigate the correlation between the long G2 of the *pot1*Δ *rqh1-hd* double mutant and its TBZ sensitivity, I examined the TBZ sensitivity of the *pot1*Δ *rqh1-hd wee1-50 mik1*Δ cells. I used *wee1-50* mutant rather than *wee1*Δ because *wee1*Δ cells diploidized at a high rate. I found that *pot1*Δ *rqh1-hd wee1-50 mik1*Δ cells are not sensitive to TBZ (Fig. 2.2A), supporting the link between the long G2 and the TBZ sensitivity of the *pot1*Δ *rqh1-hd* double mutant.

I next examined whether the telomeres in *pot1*Δ *rqh1-hd wee1-50 mik1*Δ cells are maintained by HR similar to that of the *pot1*Δ *rqh1-hd* double mutant. To this end, the genomic DNA of *pot1*Δ *rqh1-hd wee1-50 mik1*Δ cells was digested with EcoRI and analyzed by Southern blotting at 25ºC using a probe containing telomere and TAS1 DNA fragments. I found that the telomeres in the *pot1*Δ *rqh1-hd wee1-50 mik1*Δ cells show a distinct pattern of amplified TAS1 similar to that of the *pot1*Δ *rqh1-hd* double mutant (Fig.

2.2B and 2.2C), implying that the telomeres in *pot1*Δ *rqh1-hd wee1-50 mik1*Δ cells are maintained by HR.

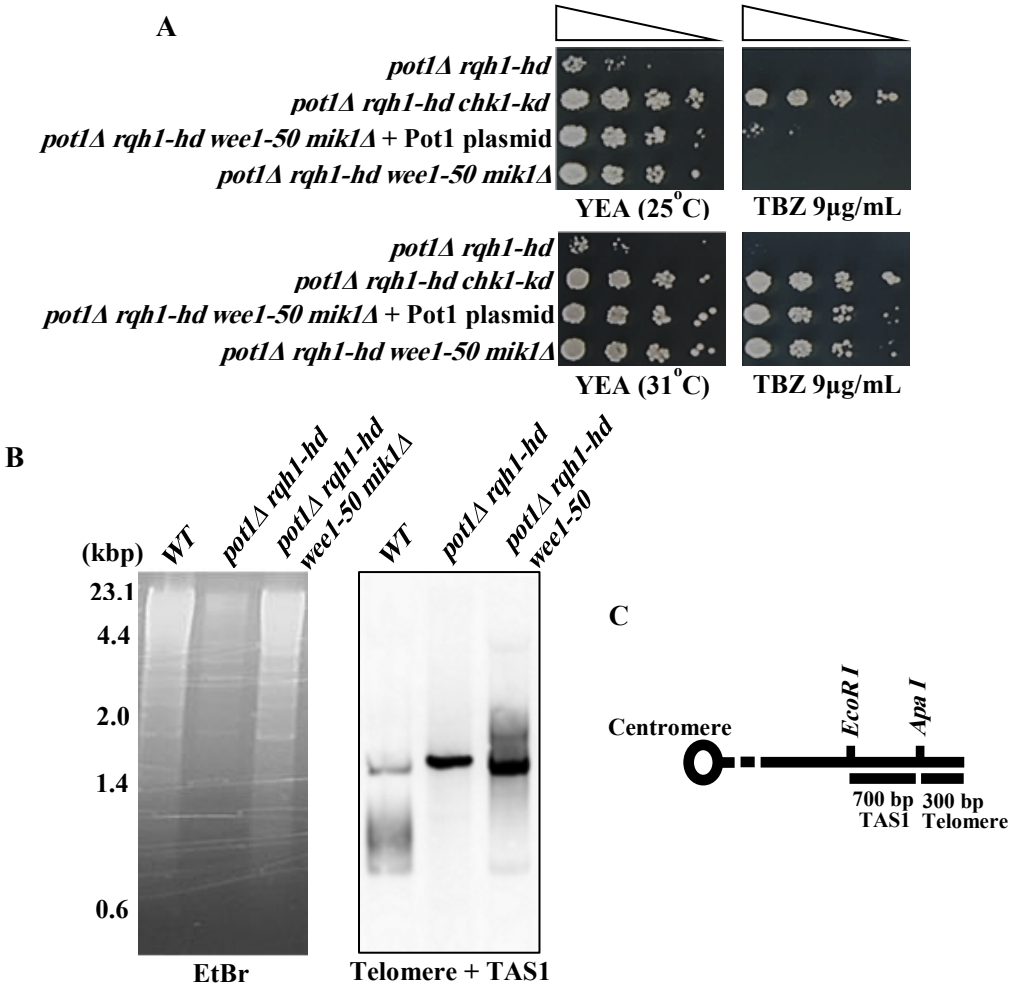

Fig. 2.2. Concomitant loss-of-function mutation of *wee1*$^+$ and *mik1*$^+$ suppressed the TBZ sensitivity of the *pot1*Δ *rqh1-hd* double mutant. (A) Spotting assay of ten-fold serial dilutions of log-phase cells. The *pot1*Δ *rqh1-hd*, *pot1*Δ *rqh1-hd chk1-kd*, *pot1*Δ *rqh1-hd wee1-50 mik1*Δ cells expressing Pot1 from a plasmid, and *pot1*Δ *rqh1-hd wee1-50 mik1*Δ mutant cells were spotted onto YEA plate and YEA plates containing 9 μg/mL TBZ at the indicated temperatures. (B) The telomere length of wild-type, *pot1*Δ *rqh1-hd*, and *pot1*Δ *rqh1-hd wee1-50 mik1*Δ cells was analyzed by Southern hybridization. Genomic DNA was digested by EcoRI, fractionated on 1.5% agarose gel electrophoresis and hybridized to a probe containing telomere fragment of 300 bp plus TAS1 of 700 bp. To assess the total amount of DNA, the gel was stained with ethidium bromide (EtBr) before blotting onto the membrane. (C) Restriction enzyme sites around the telomere and TAS1 of one chromosome arm cloned in the plasmid pNSU70.

2.3.2 The loss-of-function mutation of *wee1*$^+$ and *mik1*$^+$ suppressed the accumulation of telomeric recombination in the *pot1*Δ *rqh1-hd* double mutant

I further examined the chromosome topology in *pot1*Δ *rqh1-hd wee1-50 mik1*Δ cells by PFGE at 31^{o}C. The genomic DNA was digested with NotI and the presence of the NotI-digested chromosomal end fragments located at the termini of chromosomes I and II were analyzed. In the *pot1*Δ *rqh1-hd* double mutant, the chromosome end fragments M, L, I, and C were not observed, suggesting that the chromosome ends of that double mutant would harbor branched structure, possibly recombination intermediates and thus failed to enter the gel. This result reproduced the previous result showing that the chromosome end fragments of the *pot1*Δ *rqh1-hd* double mutant were unable to enter the gel, possibly due to the accumulation of the recombination intermediates [51]. In sharp contrast, I could detect the chromosome end fragments M, L, I, and C of *pot1*Δ *rqh1-hd wee1-50 mik1*Δ cells (Fig. 2.3A and 2.3B). This result suggests that the accumulation of the recombination intermediates is suppressed in *pot1*Δ *rqh1-hd wee1-50 mik1*Δ cells and highlights the link between long G2 and the accumulation of recombination intermediates at telomeres of the *pot1*Δ *rqh1-hd* double mutant.

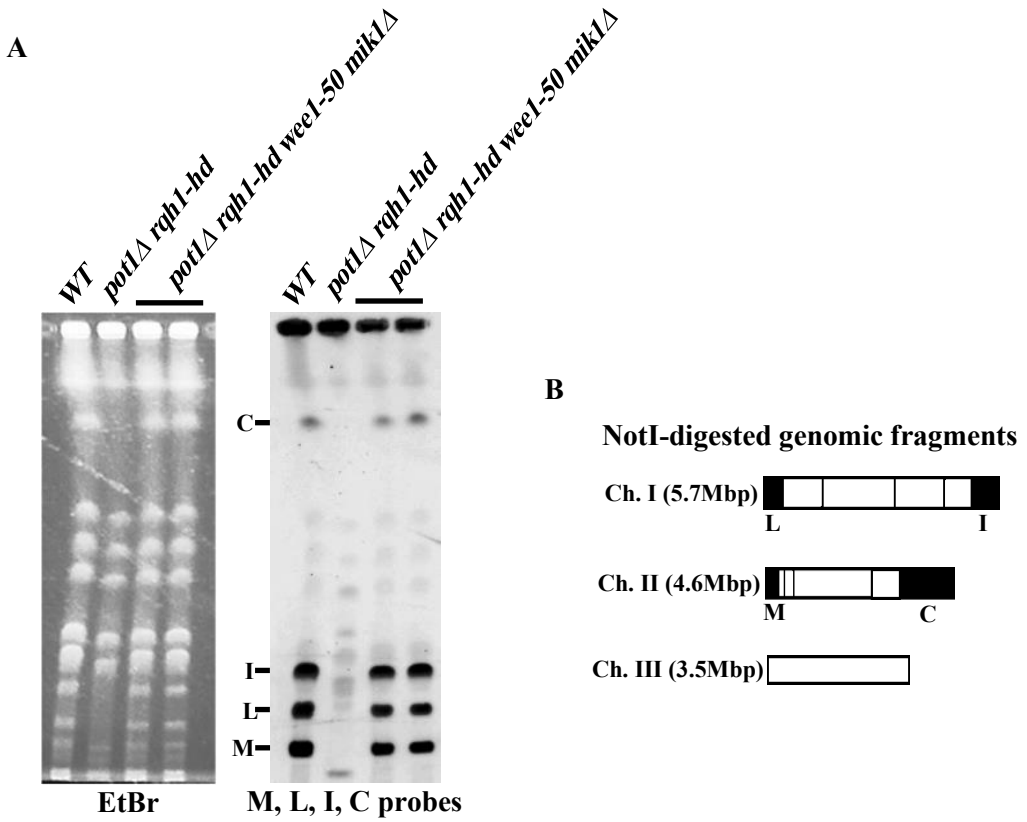

Fig. 2.3. The chromosome end fragments of *pot1*Δ *rqh1-hd wee1-50 mik1*Δ cells are linear.

(A) NotI-digested genomic DNA from wild-type and two independent colonies of *pot1*Δ *rqh1-hd wee1-50 mik1*Δ were analyzed using PFGE at 31°C. The digested DNA was separated on a 1% agarose gel and the terminal chromosomal fragments were detected using probes specific to NotI-digested fragments (M, L, I, and C). (B) NotI restriction site map of *S. pombe* chromosomes I, II, and III is shown.

2.3.3 The gain-of-function mutation of Cdc2 suppresses the TBZ sensitivity of the *pot1*Δ *rqh1-hd* double mutant

To further provide evidence supporting the link between the long G2 and the TBZ sensitivity of the *pot1*Δ *rqh1-hd* double mutant, I searched for another mutation that shortens the G2 of the *pot1*Δ *rqh1-hd* double mutant. Cdc2, together with its regulatory subunit cyclin B, is the key regulator that orchestrates the cell cycle transition [94, 95].

cdc2-3w (C67Y) is a gain function allele of Cdc2 that does not require Cdc25 for mitotic induction. *cdc2-3w* cells can bypass the checkpoint control and enter mitosis with a very small cell size compared with the wild-type [98]. Indeed, I found that *cdc2-3w* mutation shortened the G2 and decreased the cell size of *pot1*Δ *rqh1-hd* cells (Fig. 2.4A).

I next examined the TBZ sensitivity phenotype of the *pot1*Δ *rqh1-hd cdc2-3w* triple mutant cells. Interestingly, I found that *pot1*Δ *rqh1-hd cdc2-3w* cells were no longer sensitive to TBZ (Fig. 2.4B), further supporting the link between the G2 length of the *pot1*Δ *rqh1-hd* double mutant and is TBZ sensitivity.

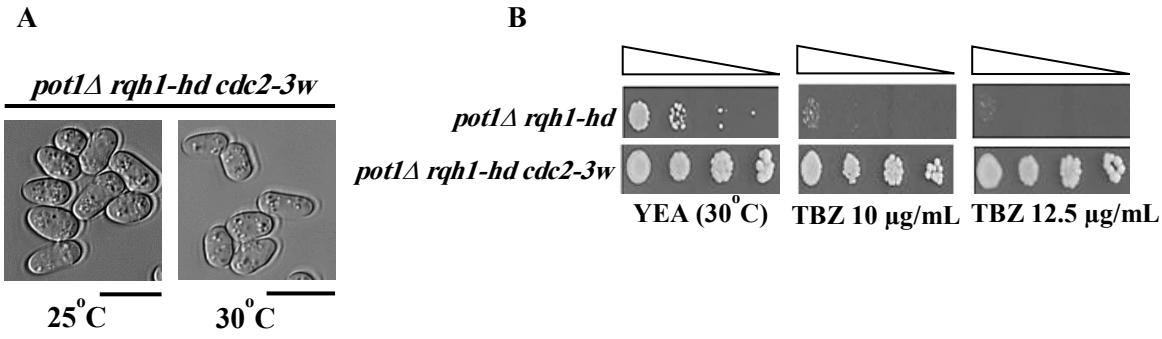

Fig. 2.4. The gain-of-function mutation of Cdc2 suppressed the TBZ sensitivity of the *pot1*Δ *rqh1-hd* double mutant. (A) The cell length of vegetative growing *pot1*Δ *rqh1-hd cdc2-3w* cells at the indicated temperatures. The scale bar represents 10 µm. (B) Spotting assay of ten-fold serial dilutions log-phase cells were spotted on YEA and YEA containing TBZ (10, and 12.5 µg/mL) at the indicated temperatures.

2.3.4 *cdc2-3w* mutation inhibits the accumulation of recombination intermediates at the telomeres of the *pot1*Δ *rqh1-hd* double mutant

I next assessed whether the *pot1*Δ *rqh1-hd cdc2-3w* triple mutant maintains telomeres by HR like the *pot1*Δ *rqh1-hd* double mutant by using Southern hybridization at 25°C as I previously described in *pot1*Δ *rqh1-hd wee1-50 mik1*Δ. The Southern

hybridization analysis revealed that *pot1*Δ *rqh1-hd cdc2-3w* cells display amplified TAS1 pattern similar to the *pot1*Δ *rqh1-hd* cells (Fig. 2.5A), implying that *pot1*Δ *rqh1-hd cdc2-3w* cells maintain telomeres by HR. I next examined whether shortening the G2 of the *pot1*Δ *rqh1-hd* cells by *cdc2-3w* mutation will suppress the accumulation of recombination intermediates at telomeres. Therefore, I treated the genomic DNA of *pot1*Δ *rqh1-hd cdc2-3w* cells with NotI and analyzed the presence of the chromosome end fragments M, L, I and C by PFGE at 25°C. Interestingly, I was able to detect the four terminal fragments M, L, I, and C (Fig. 2.5B) implying that the accumulation of recombination intermediates was suppressed at the telomeres of *pot1*Δ *rqh1-hd cdc2-3w* cells. This result again supports the link between long G2 of the *pot1*Δ *rqh1-hd* and the accumulation of recombination intermediates at telomeres.

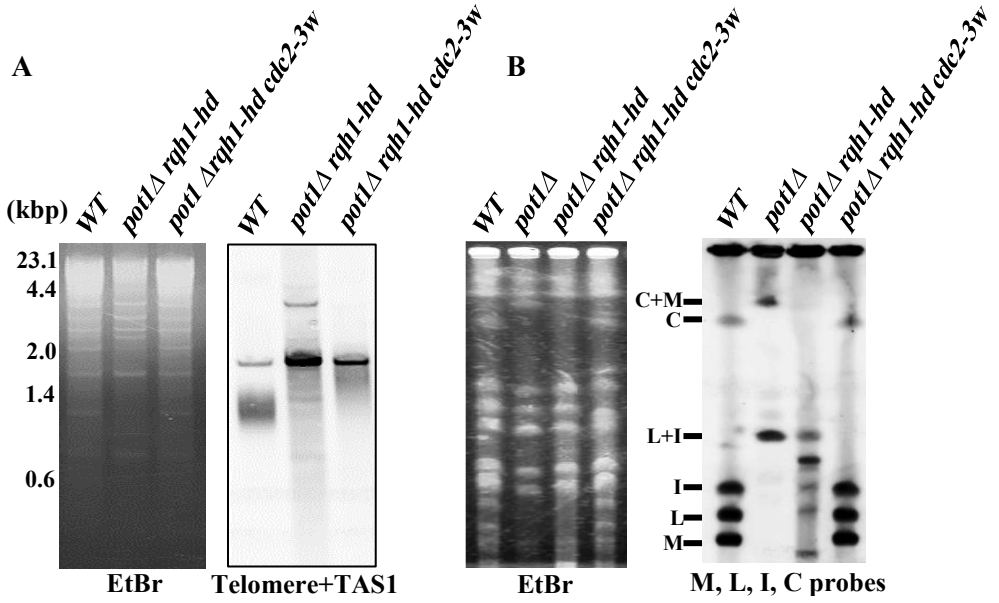

Fig. 2.5. *cdc2-3w* mutation suppresses the accumulation of recombination intermediates at the chromosome ends of the *pot1*Δ *rqh1-hd* double mutant. (A) The telomere length of wild-type, *pot1*Δ *rqh1-hd*, and *pot1*Δ *rqh1-hd cdc2-3w* mutant cells was analyzed by Southern hybridization at 25°C using a probe containing telomere fragment of 300 bp plus TAS1 of 700bp. (B) NotI-digested *S. pombe* chromosomal DNA from wild-type, *pot1*Δ, *pot1*Δ *rqh1-hd*, and *pot1*Δ *rqh1-hd cdc2-3w* cells were analyzed using PFGE at 25°C.

2.4 Summary

The fission yeast Pot1 is required for telomerase-dependent telomere maintenance [31]. Therefore, fission yeast *pot1*Δ cells exhibit rampant telomere loss followed by an intrachromosomal end-to-end fusion [30]. Fission yeast Rqh1 is important to inhibit the inappropriate recombination events since *rqh1-hd* cells show hyper-recombination phenotype [44]. Therefore, *rqh1-hd* cells can trigger recombination-mediated telomere maintenance in the absence of Pot1 [51]. In vertebra, inhibition of Pot1 activates DNA damage signaling at telomeres and induces cell cycle arrest which is Chk1-dependent [99]. Moreover, in mice, the lack-of-function of one of the two Pot1 orthologs, POT1a, elicits aberrant recombination at telomeres, suggesting the role of POT1 in the suppression of recombination events at telomeres [100]. These facts suggest that the *pot1*Δ *rqh1-hd* cells experience DNA damage checkpoint activation and accumulation of recombination structures at telomeres. Indeed, the *pot1*Δ *rqh1-hd* double mutant displays long G2 (Fig. 2.1) and telomeres are maintained by HR. A characteristic phenotype of the *pot1*Δ *rqh1-hd* cells is the sensitivity to TBZ. Interestingly, deletion of $chk1^{+}$ or mutation of its kinase domain shortened the G2 and suppressed the TBZ sensitivity of *pot1*Δ *rqh1-hd* cells (Fig. 2.1 and 2.2A) and the accumulation of recombination intermediates at telomeres, implying a link between long G2 of the *pot1*Δ *rqh1-hd* and its TBZ sensitivity.

One possible explanation is that lengthening the G2 upon activation of the DNA damage checkpoint provides a time for the recombination intermediates to accumulate at telomeres which causes segregation problem in the presence of TBZ. If this is true, then a mutation that can escape DNA damage checkpoint control should suppress the accumulation of telomeric recombination and hence the TBZ sensitivity. Indeed, I found

that *wee1-50 mik1*Δ and *cdc2-3w* mutations that bypass the DNA damage checkpoint control shortened the G2 length of the *pot1*Δ *rqh1-hd* double mutant and suppressed the TBZ sensitivity and the accumulation of recombination intermediates at telomere, supporting the link between the long G2 of the *pot1*Δ *rqh1-hd* double mutant and its TBZ sensitivity. These results suggest that the cell cycle arrest mediated by the activation of the DNA damage checkpoint can adversely affect the cells' viability by contributing to the accumulation of toxic recombination intermediates when telomere function is compromised. In line with this, deletion of DNA damage checkpoint *rad9*$^{+}$ or *chk1*$^{+}$ suppressed the G2/M arrest and the slow growth phenotype of the fission yeast *srs2*Δ *rqh1*Δ double mutant. Moreover, deletion of recombination genes *rad51*$^{+}$ or *rad57*$^{+}$ enhanced the *srs2*Δ *rqh1*Δ cells' viability, implying that the G2/M arrest is recombination-dependent and this DNA-damage checkpoint-dependent arrest worsen cells' viability [101].

Model of the mechanism of the TBZ sensitivity phenotype of the *pot1*Δ *rqh1-hd* double mutant

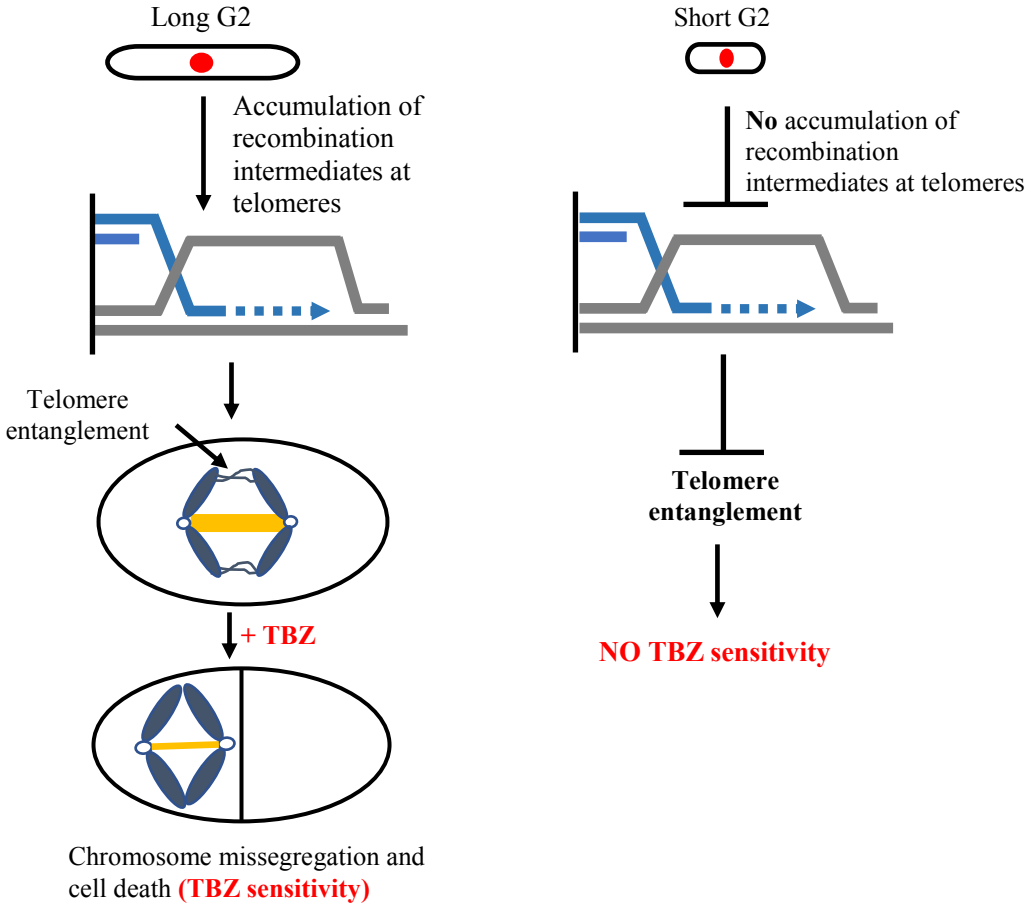

Fig. 2.6. Model of the mechanism of TBZ sensitivity phenotype of the *pot1*Δ *rqh1-hd* double mutant. The long G2 phenotype of the *pot1*Δ *rqh1-hd* double mutant allows time for the accumulation of recombination intermediates at the telomeres of the double mutant, producing entangled chromosome ends which perturb chromosome segregation in the presence of TBZ.

Chapter 3. Chromosome passenger complex is required for the survival of cells with ring chromosomes in fission yeast

Note: This study was published in PLoS One [102]. Most of the figures and tables in this chapter were reproduced from the published article with slight modifications.

3.1 Introduction

RCs are circular DNA molecules that can be formed because of breakage at both arms of chromosomes following by fusion of the chromosomal ends with the loss of some genetic materials at the broken regions [2, 53]. Alternatively, RCs can be formed due to telomere dysfunction through fusion between subtelomeric sequences, telomere-telomere or telomeric-subtelomeric regions without loss of genetic materials, generating complete ring chromosome [54]. RCs have been observed in many types of human cancers and genetic disorders with a variable frequency [53, 61, 62]. In fission yeast, chromosome circularization followed telomere resection had been observed in some mutants such as *pot1*Δ, *tpz1*Δ, *poz1*Δ *ccq1*Δ, *rad3*Δ *tel1*Δ, *rad3*Δ *MRN*Δ and *trt1*Δ cells [30, 31, 40, 103].

To date, the molecular mechanisms of the maintenance of circular chromosomes and how cells with circular chromosomes can survive are largely unknown. In this study, I attempted to understand how cells with circular chromosomes could survive by determining a gene whose dysfunction induces the death of cells with circular chromosome using a synthetic lethality approach. Synthetic lethal interaction occurs when the concomitant perturbation of the function of two genes results in cell death while the perturbation of a single gene does not affect cell survival [104].

Chromosome passenger complex (CPC) is an evolutionarily conserved protein complex composed of four subunits: the enzymatic subunit Aurora B kinase,

scaffolding subunit inner centromeric protein (INCENP), and regulatory subunits Survivin and Borealin (also known as Dasra) [105, 106]. CPC plays crucial roles in driving and regulation of various mitotic events including chromosome condensation, chromosome congression and segregation, activation of spindle assembly checkpoint, and cytokinesis [105-107]. Dysfunction of CPC leads to chromosome segregation errors and failure of cytokinesis which eventually increase the frequency of generation of aneuploid cells and chromosome instability, a hallmark of many human cancers [105-107]. To ensure the fidelity of mitosis, CPC components are dynamically distributed at different locations to regulate multiple processes at different times during mitosis. At early prophase, the CPC is localized to chromosomal arms to promote the resolution of cohesion [105-107]. During prometaphase, CPC is confined to the inner centromeric region to assist in the destabilization of incorrect kinetochore-microtubule attachment and thus activation of spindle assembly checkpoint (SAC) till establishment of correct chromosome biorientation. Upon the metaphase-to-anaphase transition, the CPC moves from the inner centromere to the spindle midzone followed by a transition to the cell equator and midbody to help in the efficient completion of cytokinesis and initiation of mitotic exit [105-107]. Additionally, Aurora B, as an enzymatic component of the CPC, plays a role in phosphorylation of histone H3 at serine 10 in many organisms which is crucial for efficient chromosome segregation [105-107]. In fission yeast, the homologs of CPC complex have been identified as Aurora B/Ark1, INCENP/Pic1, Survivin/Bir1, and Borealin/Nbl1 with localization patterns closely resemble that of mammals [108, 109].

Appropriate regulation of CPC activity is crucial to protect against genomic instability and tumorigenesis. For instance, overexpression of Aurora B has been reported in many types of cancer such as hepatocellular carcinoma, non-small cell lung

carcinoma, thyroid carcinoma, breast, and colon cancers [110-114]. Overexpression of Survivin has also been observed in most of the human tumors especially lung, colon, breast, prostate and brain cancers [115-119]. Moreover, overexpression of Aurora B and Survivin is associated with poor prognosis of some types of cancer such as ovarian, and liver cancers [120, 121]. Recently, several anti-cancer drugs that inhibit the expression of Aurora kinase B and Survivin have been developed and undergone clinical trials [122, 123].

In this study, I have investigated the importance of CPC for the survival of cells with RCs. I found that the lack of function of CPC components is lethal to fission yeast *pot1*Δ and *trt1*Δ cells with circular chromosomes. Dysfunction of CPC subunits (Pic1) in *pot1*Δ cells leads to severe growth defect and accumulation of high rates of chromosome mis-segregation and DNA damage. I further found that neither Shugoshin (Sgo2) nor heterochromatin protein (Swi6), which contribute to the centromeric localization of CPC, were required for the viability of *pot1*Δ cells. My results reveal the importance of CPC for the survival of cells with circular chromosomes and shed light on the possible roles of CPC in the maintenance of circular chromosomes.

Table 3.1 *Schizosaccharomyces pombe* strains used in this study

Strain	Genotype	Source
FY9361	*h⁻ leu1 cut17-275*	NBRP
AGK004	*h⁺ leu1-32 ura4-D18 ade6-M210 pot1::kanMX6 (pPC27-Leu1-pot1⁺-HA)*	Lab freeze stock
AGK026	*h⁻ leu1 ade6-M210 pot1::kanMX6 cut17-275 (pPC27- Leu1-pot1⁺-HA)*	This study
FY24496	*h⁹⁰ ade6-M216 leu1 bir1-T1<<kanr*	NBRP
AGK027	*h⁺ leu1-32 ura4-D18 ade6-M210 pot1::kanMX6 bir1-T1<<kanr (pPC27-Leu1- pot1⁺-HA)*	This study
FY24764	*h⁻ leu1 ade6-M216 pic1-T269<<hygR*	NBRP
SU001	*h⁺ leu1-32 ura4-D18 ade6-M216 pot1::kanMX6 pic1-T269<<hygR (pPC27-Leu1- pot1⁺-HA)*	This study
SU002	*h⁺ leu1-32 ura4-D18 ade6-M216 pot1::kanMX6 pic1-T269<<hygR*	This study
FY24593	*h⁻ leu1 ade6 ark1-T7<<kanR Z::Padh 15 mCherry-atb2⁺<<natR*	NBRP
SU005	*h⁺ leu1-32 ura4-D18 ade6 pot1::kanMX6 ark1-T7<<kanR Z::Padh 15 mCherry-atb2⁺<<natR (pPC27-Leu1- pot1⁺-HA)*	This study
FY24484	*h⁹⁰ ade6-M216 leu1 ark1-T8-GFP<<kanR*	NBRP
SU006	*h⁺ leu1-32 ura4-D18 ade6 pot1::kanMX6 ark1-T8-GFP<<kanR (pPC27-Leu1- pot1⁺-HA)*	This study
NK310	*h⁺ leu1-32 ura4-D18 ade6-M210 trt1::kanMX6 pPC96-trt1⁺*	S. Ukimori
AGK120	*h⁻ leu1 ura4-D18 ade6-M216 trt1::kanMX6 pic1-T269<<hygR pPC96-trt1⁺*	This Study
AGK121	*h⁻ leu1 ura4-D18 ade6-M216 trt1::kanMX6 pic1-T269<<hygR*	This Study
FY13784	*h⁹⁰ leu1 ade6-M210 ura4-D18 sgo2::ura4⁺*	NBRP
AGK009	*h⁺ leu1 ade6-M210 ura4-D18 pot1::kanMX6 sgo2::ura4⁺ (pPC27-Leu1-pot1⁺-HA)*	This study
AGK010	*h⁺ leu1 ade6-M210 ura4-D18 pot1::kanMX6 sgo2::ura4⁺*	This Study
FY13725	*h⁹⁰ leu1 ade6-M210 ura4-D18 swi6::ura4⁺*	NBRP
AGK014	*h⁺ leu1 ade6-M210 ura4-D18 pot1::kanMX6 swi6::ura4⁺ (pPC27-Leu1-pot1⁺-HA)*	This study
AGK015	*h⁺ leu1 ade6-M210 ura4-D18 pot1::kanMX6 swi6::ura4⁺*	This Study
TN004	*h⁺ rad11-mRFP::natMX6*	T. Nanbu
KTA038	*h⁻ leu1-32 ura4-D18 ade6 pot1::kanMX6 rad11-mRFP::natMX6*	T. Nanbu
SU003	*h⁻ leu1 ade6-M216 pic1-T269<<hygR rad11-mRFP::natMX6*	This study
SU004	*h⁺ leu1-32 ura4-D18 ade6-M216 pot1::kanMX6 pic1-T269<<hygR rad11-mRFP::natMX6*	This study
AGK089	*h⁹⁰ leu1 ade6-M210 ura4-D18 sgo2::ura4⁺ rad11-mRFP::natMX6*	This Study
AGK090	*h⁹⁰ leu1 ade6-M210 ura4-D18 swi6::ura4⁺ rad11-mRFP::natMX6*	This Study
AGK091	*h⁺ leu1 ade6-M210 ura4-D18 pot1::kanMX6 sgo2::ura4⁺ rad11-mRFP::natMX6*	This Study
AGK092	*h⁺ leu1 ade6-M210 ura4-D18 pot1::kanMX6 swi6::ura4⁺ rad11-mRFP::natMX6*	This Study

3.2 Materials and methods

3.2.1 Strain construction

The *pot1*Δ *cut17-275* (*pot1::kanMX6 cut17-275*), *pot1*Δ *bir1-T1* (*pot1::kanMX6 bir1-T1*), *pot1*Δ *pic1-T269* (*pot1::kanMX6 pic1-T269*), *pot1*Δ *ark1-T7* (*pot1::kanMX6 ark1-T7*), and *pot1*Δ *ark1-T8* (*pot1::kanMX6 ark1-T8*) double mutants expressing Pot1 from the plasmid (pPC27- pot1^{+}-hemagglutinin [HA], containing *leu1*$^{+}$) were constructed by mating *h*$^{-}$ *leu1 cut17-275*, *h*^{90} *leu1 ade6-M216 bir1-T1<<kanr, h*$^{-}$ *leu1 ade6-M216 pic1-T269<<hygR, h*$^{-}$ *leu1 ade6 ark1-T7<<kanR Z::Padh 15 mCherry-atb2*$^{+}$*<<natR* and *h*^{90} *leu1 ade6-M216 ark1-T8-GFP<<kanR*, respectively, with *h*$^{+}$ *leu1-32 ura4-D18 ade6-M210 pot1::kanMX6* expressing Pot1 from the plasmid pPC27-leu1-pot1^{+}-HA. Cells were streaked on EMM plates lacking leucine to select cells that retain the Pot1 plasmid and on YEA plates containing G418 disulfide at 25ºC to select cells that harbor *pot1::kanMX6* mutation. Candidates were then re-streaked on YEA plates at 36ºC to select for *cut17-275*, *bir1-T1*, *pic1-T269*, *ark1-T7*, and *ark1-T8* respectively. *pot1*Δ cells that could grow on YEA plates at 25ºC but not at 36ºC were selected as a double mutant.

The *trt1*Δ *pic1-T269* (*trt1::kanMX6 pic1-T269*) double mutants expressing *trt1*$^{+}$ from a plasmid were constructed by mating *h*$^{+}$ *trt1::kanMX6* cells (NK310) expressing Trt1 from the plasmid (pPC96-*trt1*$^{+}$, a gift from Professor Toru Nakamura, containing *ade6*$^{+}$ and *HSV-tk*$^{+}$ as a positive and negative selection marker, respectively) with *h*$^{-}$ *pic1-T269* (FY24764). Cells were streaked on EMM plates lacking adenine to select cells that retain the Trt1 plasmid and on YEA plates containing G418 disulfide at 25ºC to select cells that harbor *trt1::kanMX6* mutation. Cells were then re-streaked on YEA plates at 36ºC to select for *pic1-T269* mutation. *trt1::kanMX6* cells that could grow at 25ºC but not at 36ºC were selected as a double mutant. To force the loss of either Pot1

or Trt1 plasmid, the double mutants were streaked on YEA plates containing 100 μM FUDR.

*pot1*Δ *sgo2*Δ (*pot1::kanMX6 sgo2::ura4*) and *pot1*Δ *swi6*Δ (*pot1::kanMX6 swi6::ura4*) double mutants containing the Pot1 plasmid (pPC27- pot1^{+}- hemagglutinin [HA], containing *leu1*$^{+}$) were constructed by mating h^{+} *pot1::kanMX6* expressing Pot1 from the plasmid pPC27-leu1-pot1^{+}-HA with h^{90} *leu1 ade6-M210 ura4-D18 sgo2::ura4*$^{+}$ and h^{90} *leu1 ade6-M210 ura4-D18 swi6::ura4*$^{+}$, respectively. Cells were streaked on EMM plates lacking leucine and uracil to select cells that retain the Pot1 plasmid and *sgo2::ura4*$^{+}$ (in the case of *pot1*Δ *sgo2*Δ) and *swi6::ura4*$^{+}$ (in the case of *pot1*Δ *swi6*Δ). Cells were then re-streaked on YEA plates containing G418 disulfide to select cells with *pot1::kanMX6* mutation.

To tag the Rad11 protein with a monomeric red fluorescent protein (mRFP) at the C-terminus, pFA6a-mRFP-natMX6-rad11 was linearized by NspV and used in the transformation of *WT*, *pic1-T269*, *pot1*Δ, *pot1*Δ *pic1-T269*, *sgo2*Δ, *swi6*Δ, *pot1*Δ *sgo2*Δ, *pot1*Δ *swi6*Δ cells. The transformation was performed either by lithium acetate transformation method or direct transformation using *S. pombe* Direct Transformation Kit.

Lithium acetate transformation method

Ten milliliters of cell culture were grown in EMM medium with required supplements to reach a cell density of 0.5-1×10^{7} cells/mL (OD_{595} 0.2-0.5). Harvest the cells by centrifugation at 3000 rpm for 5 min. Wash the cell pellets with 40 mL sterile water and centrifuge again at 3000 rpm for 5 min. Re-suspend the cell pellets with 0.1 M lithium acetate [pH 4.9] to reach a cell density of 1×10^{9} cells/mL. Transfer the cell suspension to an Eppendorf tube and incubate at 30^{o}C for 60 min. Add 1 μg plasmid DNA dissolved in 15 μL sterile TE [pH 7.5] and mix by gentle vortex till completely

re-suspend the cells. Add 290 µL 50% (w/v) pre-warmed polyethylene glycol 4000 (PEG 4000) and mix by gentle vortex. Re-incubate the cells at 30°C for 60 min. Expose the cells to heat shock at 43°C for 15 min. Allow the tube to cool down at the room temperature for 10 min. Centrifuge the cells at 5000 rpm for 2 min. Carefully discard the supernatant and re-suspend the cell pellets in 100 µL sterile water and mix by pipetting. Spread the cells on YEA plates and incubate at 30°C for 24 h. Replica plate the cells on selective media and wait for the formation of colonies (it takes about 4 to 5 days to see the transformed cells).

Direct transformation method

Grow two to three mL of cell culture in YEA medium to reach a cell density of 0.5-1×10^7 cells/mL. Transfer 1 mL of cell culture to 1.5 mL Eppendorf tube and centrifuge at 4000 rpm for 3 min. Re-suspend the cell pellets to reach a total volume of 25 µL cell suspension. In new Eppendorf tube, prepare 100 µL of plasmid/reagent solution by adding 6 µL of 1 µg DNA insert, and 4 µL of Carrier DNA to 90 µL of *Sp.* Transformation Reagent and mix by vortexing. Transfer the 25 µL suspended yeast cells to the 100 µL plasmid/reagent solution and mix by vortexing then incubate the mixture at 37°C for 2 h. Centrifuge the cells at 4000 rpm for 3 min and re-suspend the cell pellets in 100 µL sterile water. Spread the cell suspension on YEA plates and incubate at 30°C for 24 h followed by replica plating the cells on selective media (it takes about 4-5 days to see the transformed cells).

3.2.2 Measurement of telomere length (same as described in chapter 2)

3.2.3 Pulsed-field gel electrophoresis (PFGE) (same as described in chapter 2)

3.2.4 Microscopy (same as described in chapter 2)

3.2.5 Lactose gradient synchronization

One hundred milliliters of cell culture was grown in YEA to mid-log phase (5×10^6 cells/mL) at 25ºC. Ten milliliters of 20% lactose solution was prepared in a 15 mL Falcon tube, frozen at -80ºC for 4 h, and then thawed without disturbance for 3 h at 30ºC to generate a 10-30% gradient. Cells were harvested by centrifugation at 3000 rpm for 3 min, and the cell pellets were re-suspended in 750 µL of sterile water. The cell suspension was layered on top of the lactose gradient using cut-off blue tips and centrifuged at 1000 rpm for 8 min, during which the cells formed a smear about half-way down the gradient. Fractions of about 0.1-0.4 mL were quickly removed from just below the top of the smear using cut-off blue tips. The cells were harvested by centrifugation at 4000 rpm for 30 sec in an Eppendorf tube, re-suspended in YEA medium, and examined under the microscope for the uniformly small early G2 cells.

3.3 Results

3.3.1 Pot1 is synthetically lethal with CPC subunits

Deletion of *pot1*$^+$ gives rise to cells that can survive only through chromosome circularization [30]. Therefore, I used *pot1*Δ cells to explore a gene that is required for the maintenance of a circular chromosome and thereby the survival of cells with circular chromosomes. To determine whether CPC is required for the survival of cells with circular chromosomes, I generated double mutation between Pot1 and CPC components as follow; *pot1*Δ *cut17-275*, *pot1*Δ *bir1-T1*, *pot1*Δ *ark1-T7*, *pot1*Δ *ark1-T8,* and *pot1*Δ *pic1-T269* and examined the ability of these double mutants to survive. *Cut17-275*, *bir1-T1*, *ark1-T7*, *ark1-T8*, *pic1-T269* are temperature-sensitive mutant alleles of CPC subunits since CPC is essential for cell viability. The permissive temperature of these

temperature-sensitive mutants was 25ºC. The restrictive temperature for *cut17-275*, *bir1-T1*, and *pic1-T269* was 36ºC, and for *ark1-T7* and *ark1-T8* was 33ºC (Fig. 3.1).

Given that the cells with circular chromosomes are defective in meiosis [103], the *pot1*Δ *CPC* double mutants were generated by a strategy of mating the *pot1*Δ cells expressing Pot1 from a plasmid with CPC subunits; then the cells are forced to lose the plasmid using a counter-selective medium. The Pot1 plasmid has tk^+ gene, which is used as a marker for counter-selection of the cells that could grow after the loss of the Pot1 plasmid. The expression of tk^+ in the presence of FUDR is lethal to yeast cells [124]. Therefore, FUDR-containing plates were used to select cells that able to grow after the loss of the plasmid. I found that *pot1*Δ *cut17-275*, *pot1*Δ *bir1-T1*, *pot1*Δ *ark1-T7*, *pot1*Δ *ark1-T8* double mutants lost the ability to grow after the loss of the Pot1 plasmid even at 25ºC (Fig. 3.2). The *pot1*Δ *pic1-T269* double mutant cells could produce few colonies at 25ºC. However, the cells completely lost the viability at 30ºC (Fig. 3.2). These results suggest a synthetic lethal interaction between Pot1 and CPC components and highlight the importance of CPC for the viability of cells with ring chromosomes.

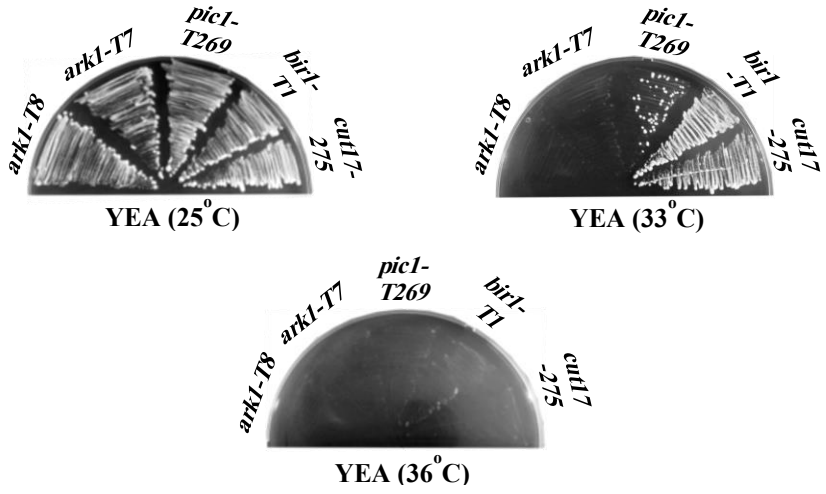

Fig. 3.1. Cell growth of the temperature-sensitive mutant alleles of CPC (*cut17-275*, *bir1-T1*, *pic1-T269, ark1-T7,* and *ark1-T8*) on YEA at the indicated temperatures.

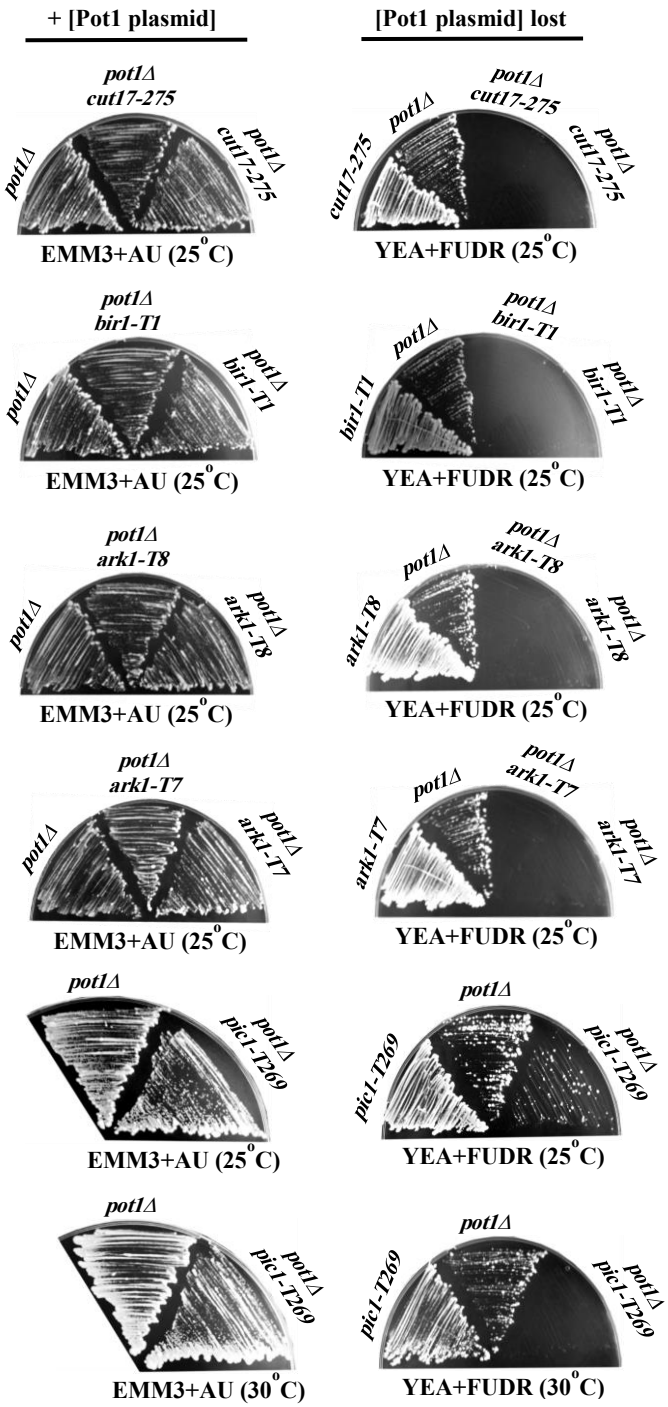

Fig. 3.2. Survival of the double mutants in the presence and absence of the Pot1 plasmid.

The *pot1*Δ *cut17-275*, *pot1*Δ *bir1-T1*, *pot1*Δ *ark1-T8*, *pot1*Δ *ark1-T7* and *pot1*Δ *pic1-T269* double mutants carrying a plasmid expressing *pot1*$^{+}$ and *tk*$^{+}$ were streaked on selective and counter-selective media at the indicated temperatures. The Pot1 plasmid was retained on EMM plates with adenine and uracil (EMM+AU). FUDR-containing plates were used as a counter-selection to examine the ability of the double mutants to grow after the loss of the Pot1 plasmid.

3.3.2 *pot1*Δ *pic1-T269* double mutant survivors have lost telomeric DNA and harbored circular chromosomes

I next examined whether the *pot1*Δ *pic1-T269* double mutant that could grow at 25ºC harbored circular chromosomes like the parental *pot1*Δ single mutant. To this end, the genomic DNA of the *pot1*Δ *pic1-T269* cells were digested by EcoRI and assessed for the loss of telomeric DNA by Southern hybridization at 25ºC using a probe containing telomere and telomere-associated sequence 1 (TAS1). I found that *pot1*Δ *pic1-T269* cells show no hybridization signal, indicating the loss of telomeric DNA as observed in *pot1*Δ cells (Fig. 3.3A and 3.3B).

I further analyzed the chromosome structure by PFGE of NotI-digested chromosomes to confirm that *pot1*Δ *pic1-T269* cells maintain the circular chromosome phenotype. Treatment of genomic DNA with NotI produces four terminal fragments (L, I, M, and C) from the telomeric DNA of Chr. I and II (Chr. III lacks NotI restriction site). Hybridization with a probe specific to these terminal fragments revealed an intrachromosomal fusion (L+I) and (C+M), band patterns reminiscent to that of circular chromosomes, indicating that the *pot1*Δ *pic1-T269* double mutant harbors circular chromosomes (Fig. 3.3C and 3.3D).

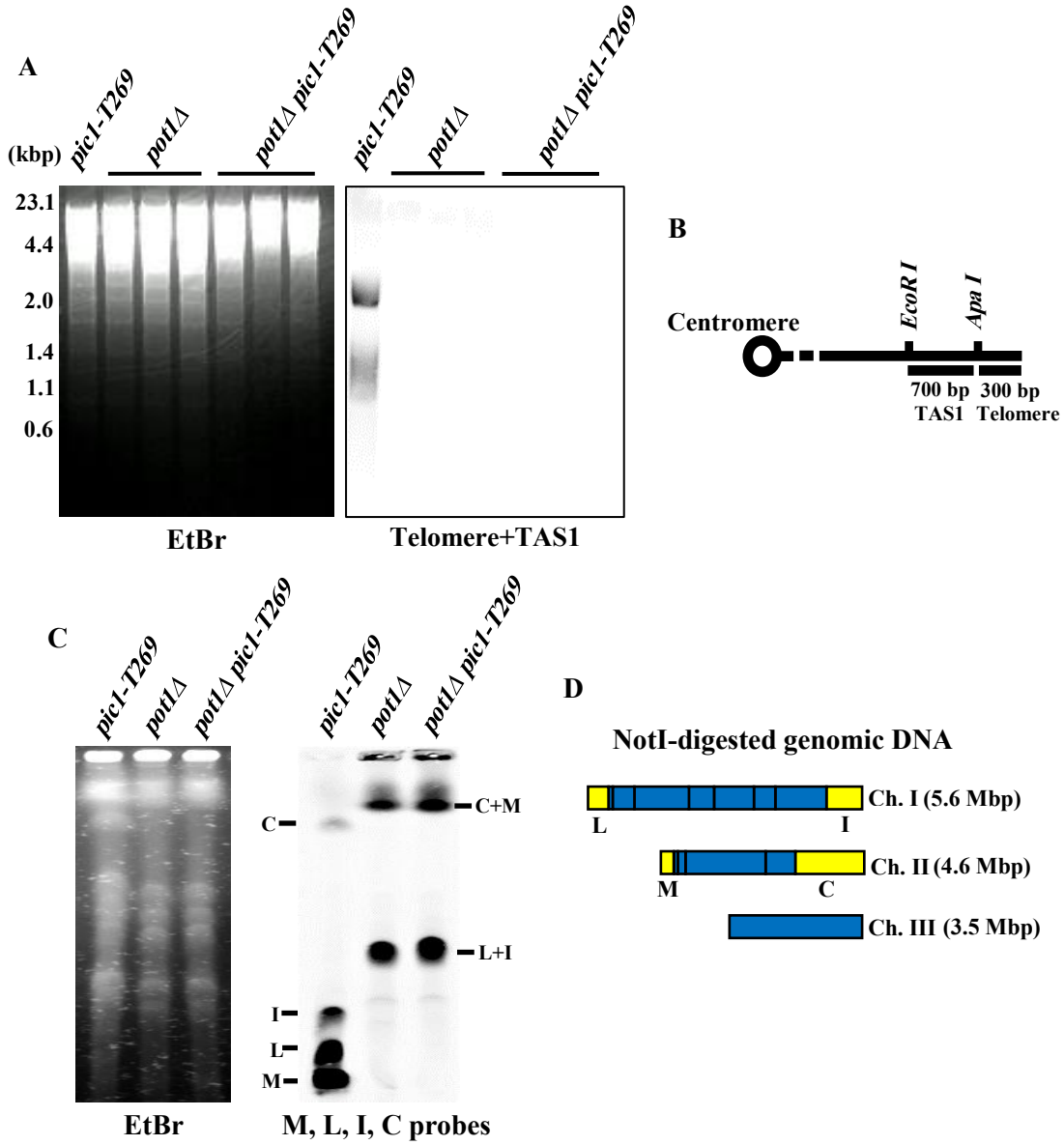

Fig. 3.3. *pot1*Δ *pic1-T269* double mutants lose telomeric DNA and chromosomes are circularized.

(A) The telomere length of *pot1*Δ *pic1-T269* double mutants was analyzed by Southern blot at 25ºC. Genomic DNA of *pic1-T269* and three independent *pot1*Δ and *pot1*Δ *pic1-T269* isolates was digested by EcoRI and fractionated by 1.5% agarose gel electrophoresis. For detection of telomeric repeats, a probe containing telomere plus telomere-associated sequence 1 (TAS1) derived from pNSU70 was used. To assess the total amount of DNA, the gel was stained with ethidium bromide (EtBr) prior to blotting onto a nylon membrane. (B) Restriction enzyme sites around the telomere and TAS1 of one chromosome arm cloned in the plasmid pNSU70. (C) NotI-digested chromosomal DNA from *pic1-T269*, *pot1*Δ , and *pot1*Δ *pic1-T269* cells were analyzed by PFGE at 25ºC. The digested DNA fractionated in a 1% agarose gel, transferred to a nylon membrane and hybridized to a mixture of probes specific to the terminal fragments (L, I, C, M). (D) NotI restriction enzyme map of *S. pombe* chromosomes.

3.3.3 Pic1 is required for the survival of *trt1*Δ cells having circular chromosomes

An intriguing question arises from the observation of the synthetic lethality of *pot1*Δ *CPC* double mutant is whether this lethality is Pot1 specific or it is a prevailing phenotype for other mutants with circular chromosomes. To test this, I should examine the synthetic lethal interaction between Pot1 and a different mutant with circular chromosomes. Deletion of fission *trt1*$^{+}$ leads to gradual telomere resection producing a population of cells that can survive via chromosome circularization [40]. Therefore, *trt1*Δ cells can be used as a model for another mutant with the circular chromosome. Since only *pot1*Δ *pic1-T269* double mutant could produce colonies at 25^{o}C, I tested the synthetic lethality of the *trt1*Δ *pic1-T269* double mutant. To this end, I constructed *trt1*Δ *pic1-T269* double mutant harboring a plasmid expressing *trt1*$^{+}$, as well as *tk*$^{+}$ to select for the cells that could grow after plasmid loss using FUDR-containing plates. I found that *trt1*Δ *pic1-T269* cells could form few colonies at 25^{o}C (Fig. 3.4A).

Given that *trt1*Δ cells can alternatively maintain telomeres via HR [40], I analyzed the loss of telomeric DNA and chromosome circularization in *trt1*Δ *pic1-T269* survivors using Southern hybridization and PFGE at 25^{o}C, respectively as previously described in the *pot1*Δ *pic1-T269* double mutant. The EcoRI-digested genomic DNA of the *trt1*Δ *pic1-T269* double mutants revealed that some of the *trt1*Δ *pic1-T269* cells lacked telomeric sequence (Fig. 3.4B). Furthermore, the PFGE analysis of the NotI-digested chromosomal DNA of these cells shows that the individual chromosome end fragments are replaced by bands corresponding to the sum of C+M and L+I, reflecting the chromosomal patterns of cells with circular chromosomes and indicating that *trt1*Δ *pic1-T269* double mutant cells have circular chromosomes (Fig. 3.4C).

I next examined the ability of these *trt1*Δ *pic1-T269* cells harboring circular chromosomes to grow at the semi-permissive temperature of 33^{o}C, the temperature at

which Pic1 partially loses its function. I found that *trt1*Δ *pic1-T269* cells failed to grow at 33°C (Fig. 3.4D), demonstrating that *trt1*Δ *pic1-T269* double mutant is also synthetically lethal.

Taken together, these results rule out the possibility that the synthetic lethality between Pot1 and CPC is Pot1-specific and affirm the importance of CPC for the survival of cells with circular chromosomes in general.

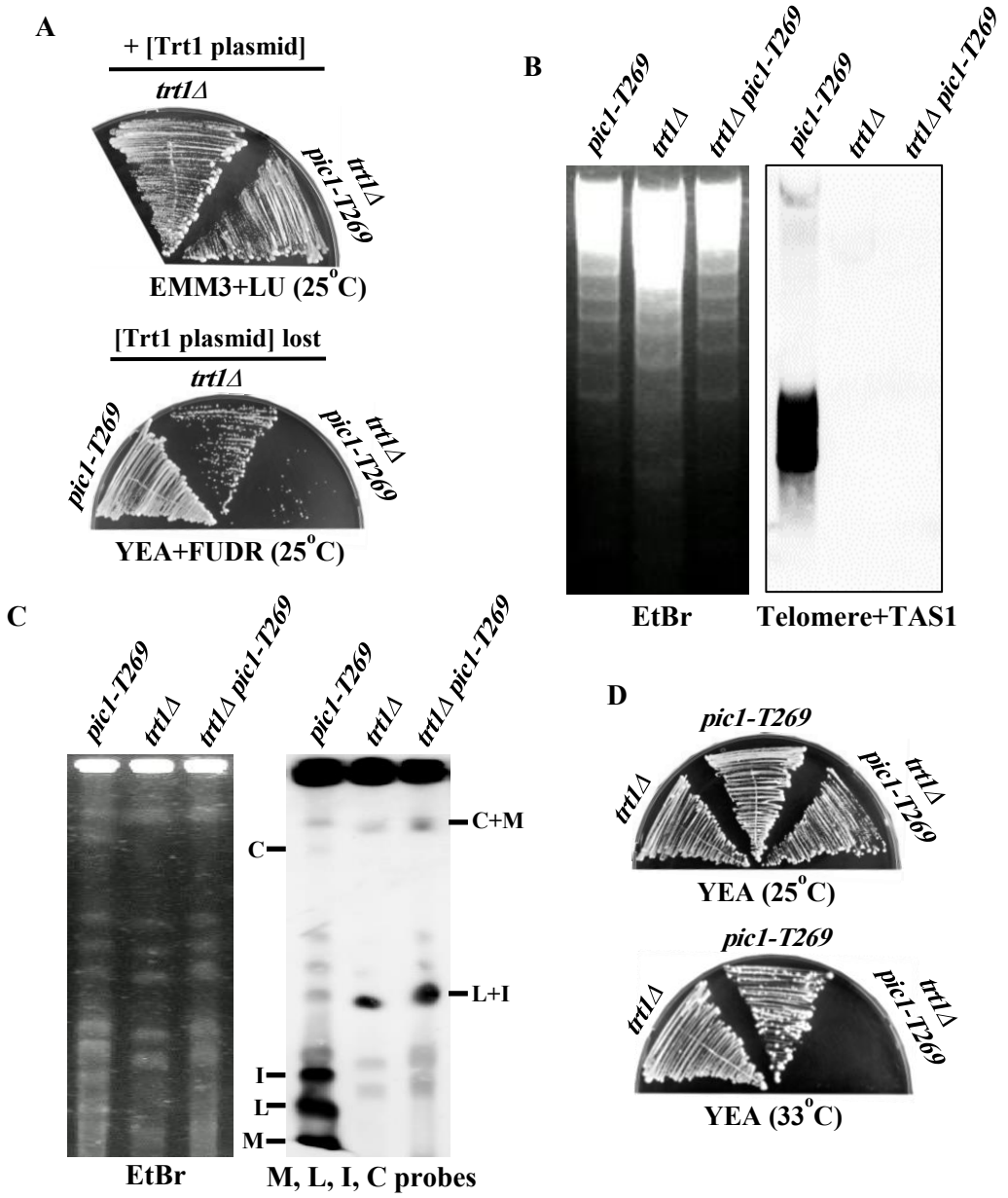

Fig. 3.4. Pic1 is required for the survival of *trt1*Δ cells with circular chromosomes.

(A) *trt1*Δ *pic1-T269* cells harbor a plasmid expressing $trt1^+$ and tk^+ were streaked on YEA+FUDR plates to select for cells that could grow after the loss of the plasmid. The plasmid was retained on EMM plates supplemented with leucine and uracil (EMM+LU). (B) *trt1*Δ *pic1-T269* double mutants lost telomeric DNA. The loss of telomeric repeats in *trt1*Δ *pic1-T269* double mutant survivors was analyzed by Southern blot at 25°C. (C) The chromosome structure of NotI-digested chromosomal DNA from *pic1-T269*, *trt1*Δ, and *trt1*Δ *pic1-T269* cells were analyzed by PFGE at 25°C. (D) Dysfunction of Pic1 leads to the death of *trt1*Δ cells with circular chromosomes. *trt1*Δ *pic1-T269* double mutant cells harbor circular chromosomes were streaked on YEA plates at 33°C to evaluate the ability of the cells to grow upon inhibiting the function of Pic1.

3.3.4 *pot1*Δ *pic1-T269* double mutant loses viability with time and displays high frequency of chromosome mis-segregation defects and DNA damage foci at 33°C

Since *pot1*Δ *pic1-T269* double mutant but not *pic1-T269* single mutant lost the viability at 33°C (Fig. 3.5A), I followed the change of growth profile of *pot1*Δ *pic1-T269* compared with *pot1*Δ and *pic1-T269* single mutants in liquid culture at 33°C. The growth in liquid culture can provide a more quantitative view to detect a subtle change in cell growth. By temperature shift to 33°C, the Pic1 partially loses its function. Therefore, if functional Pic1 is required for the survival of cells with circular chromosomes, I would observe a defect in the growth of *pot1*Δ *pic1-T269* double mutant at 33°C. To test this, I incubated *WT*, *pot1*Δ, *pic1-T269* and *pot1*Δ *pic1-T269* cells overnight at 25°C and then an equal number of cell density of each strain was shifted to 33°C for 3h. I found that *pot1*Δ *pic1-T269* cells showed a marked growth defect compared with *pot1*Δ and *pic1-T269* single mutants (Fig. 3.5B), implying that the functional Pic1 is crucial for the survival of cells with circular chromosomes.

Next, to understand the reason behind the synthetic lethality of *pot1*Δ *pic1-T269* double mutant, I investigated the phenotypes associated with the lack of function of Pic1 in *pot1*Δ cells, as a representative of cells with circular chromosomes. A characteristic phenotype associated with the dysfunction of CPC is the high frequency of chromosome mis-segregation events. Moreover, some studies reported a correlation between chromosome mis-segregation and the occurrence of DNA damage [125, 126]. According to this, I investigated whether the elevated rates of chromosome mis-segregation and DNA damage are the reason for the synthetic lethality observed in the *pot1*Δ *pic1-T269* double mutant at 33°C. To this end, I tagged Rad11, which encodes for the large subunit of replication protein A (RPA) with a monomeric red fluorescent protein (mRFP) and used it as a marker for concomitant monitoring of chromosome

segregation and DNA damage. RPA is an indicative marker of the single-stranded DNA generated during DNA replication, recombination and damage repair [127]. I incubated *WT*, *pot1*Δ, *pic1-T269*, *pot1*Δ *pic1-T269* cells expressing Rad11-mRFP overnight at 25ºC and then shifted the cells to 33ºC for 3h. I calculated the percentage of the chromosome mis-segregation and the DNA damage foci of each strain at 25ºC and 33ºC. I observed that *pot1*Δ *pic1-T269* double mutant displayed a high percentage of chromosome mis-segregation and DNA damage foci compared with *pot1*Δ and *pic1-T269* single mutants even at 25ºC (Fig. 3.5C and 3.5D).

This result implies that the synthetic lethality observed in the *pot1*Δ *pic1-T269* double mutant may be attributed to the elevated rates of chromosome segregation defects and DNA damage.

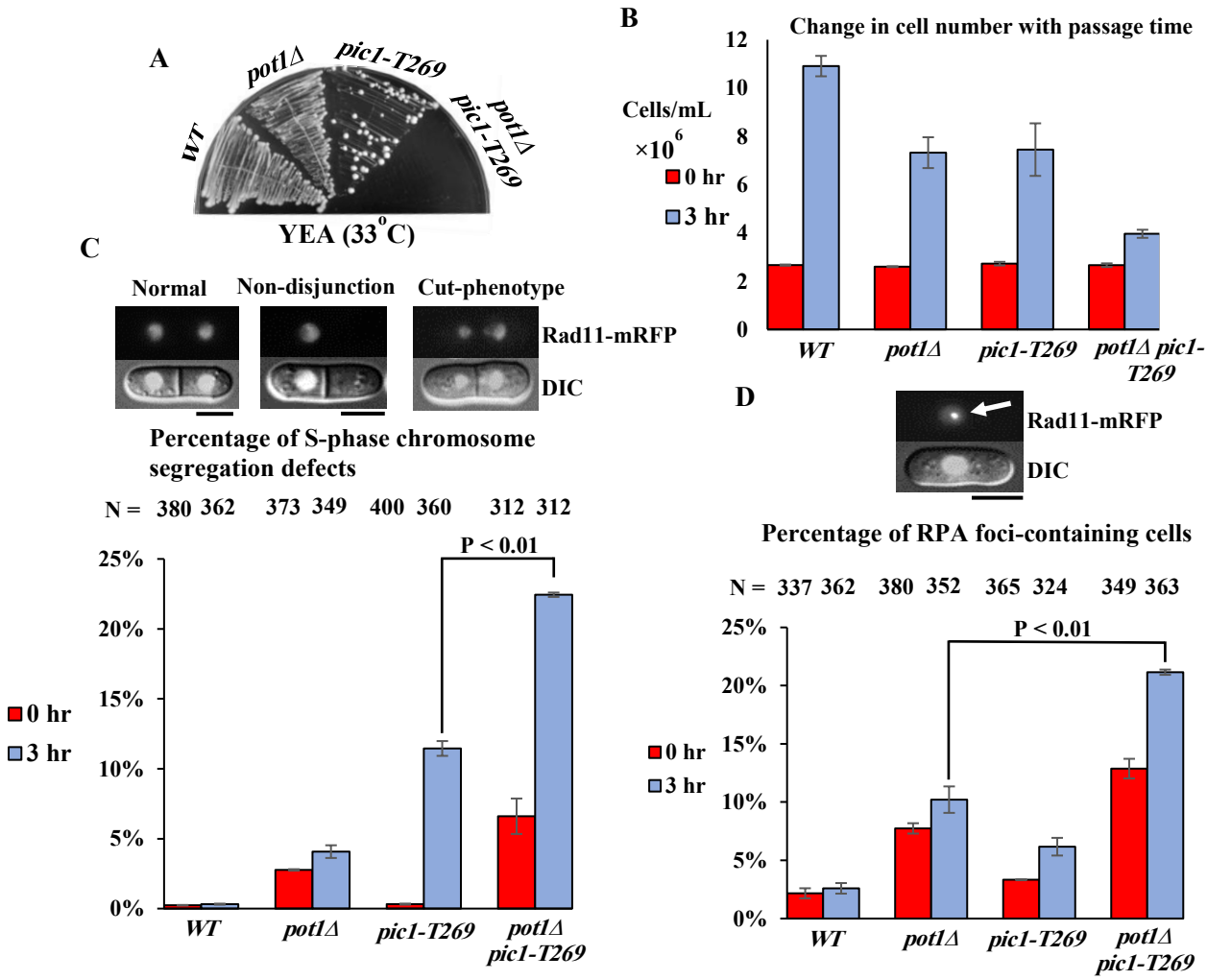

Fig. 3.5. Analysis of the synthetic lethality phenotypes associated with the lack of function of Pic1 in *pot1*Δ cells. (A) *pot1*Δ *pic1-T269* double mutant cells lost viability at a semi-permissive temperature (33ºC). (B) Change in the cell number with time at 33ºC. *WT*, *pot1*Δ, *pic1-T269*, and *pot1*Δ *pic1-T269* cells were cultured overnight in YEA at 25ºC. An equal number (2.62×10^6 cells/mL) of each strain was shifted to 33ºC and incubated for 3 h. The difference in the cell number after 3 h temperature shift was measured using a hemocytometer. Error bars indicate standard deviation (SD) of three replicates (n = 3). (C) The percentage of chromosome segregation errors of septating asynchronous *WT*, *pot1*Δ, *pic1-T269*, and *pot1*Δ *pic1-T269* cells expressing Rad11 endogenously tagged with mRFP at 25ºC and after 3 h incubation at 33ºC. Examples of cells with chromosome segregation errors such as cut-phenotype and chromosome non-disjunction are shown on the top. (D) The percentage of RPA foci-containing cells at 25ºC and after the 3 h temperature shift to 33ºC using the data from chromosome segregation defects analysis. Arrow marks the RPA foci. N in the top represents the number of cells examined. Error bars indicate standard deviation (SD) of three replicates (n = 3). The scale bar = 5 µm.

3.3.5 The formation of RPA foci in *pot1*Δ *pic1-T269* double mutant does not directly link to chromosome mis-segregation events

I next asked whether there is a link between the high rates of chromosome segregation errors and the DNA damage foci observed in the *pot1*Δ *pic1-T269* double mutant at 33ºC. To test this, I monitored the percentage of chromosome mis-segregation and the DNA damage foci at each stage of the cell cycle by using lactose gradient synchronization method that synchronizes the cells at early G2 marked with small-sized cells with one nucleus. I cultured the *pot1*Δ *pic1-T269* cells expressing Rad11-mRFP at 25ºC then the synchronized cells were shifted to 33ºC, sampled every 20 min (Fig. 3.6) and examined for the percentage of DNA damage and chromosome mis-segregation. I found that the RPA foci are mostly present in G2 cells and the percentage of RPA foci did not increase in proportion to the increase in the percentage of M and S-phase cells with chromosome segregation errors (Fig. 3.7A). This implies that chromosome mis-segregation does not directly induce the generation of DNA damage in S-phase.

I next sought to examine whether the existence of RPA foci in G2 would induce chromosome segregation errors by counting the percentage of M-phase cells with chromosome mis-segregation that has RPA foci. I found that a very small percentage (~ 5%) of the M-phase cells with chromosome mis-segregation had DNA damage (Fig. 3.7B), excluding the possibility that the generation of DNA damage in G2 causes chromosome mis-segregation. Furthermore, to evaluate the possibility that tearing the mis-segregated chromosomes that entrapped at the cleavage furrow by septum during cytokinesis leads to the generation of DNA damage foci, I scored the percentage of septating cells with chromosome mis-segregation that had RPA foci. I found that a low fraction (~10%) of septating cells with chromosome mis-segregation displayed RPA

foci (Fig. 3.7C), implying that cytokinesis does not induce DNA damage in S-phase, where the DNA damage is active.

Collectively, these results indicate that the RPA foci formation in the *pot1*Δ *pic1-T269* double mutant does not directly correlate with the chromosome mis-segregation events.

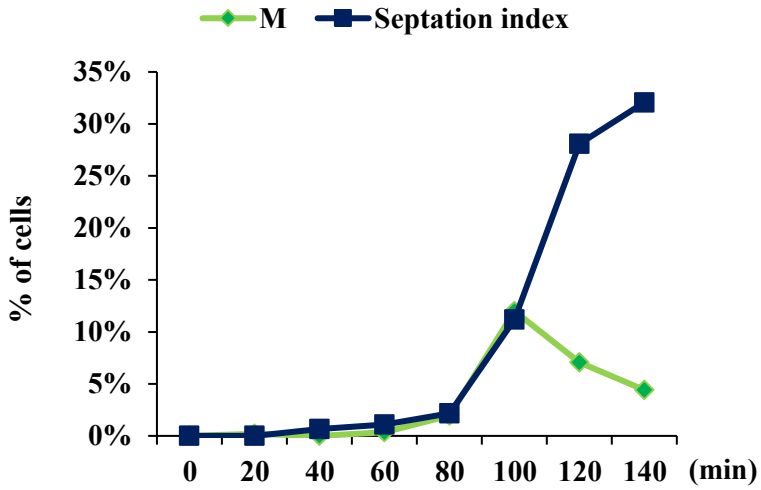

Fig. 3.6. Cell cycle progression of the *pot1*Δ *pic1-T269* double mutant. Synchronous early G2 cells accumulated using lactose gradient centrifugation and progression through the cell cycle was monitored by sampling the cells every 20 min after temperature shift to 33°C. The percentages of M-phase (two nuclei without septum) and S-phase (two nuclei with septum) cells are shown.

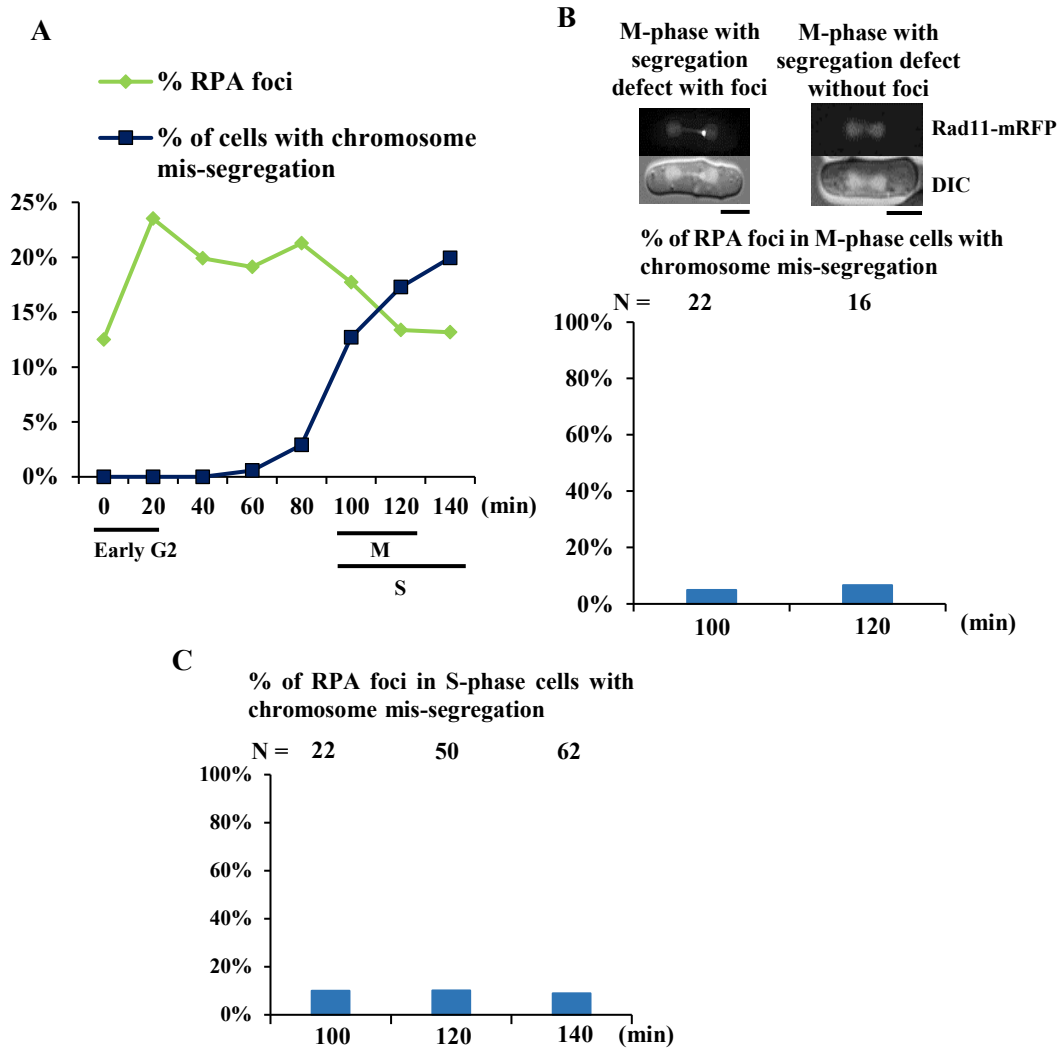

Fig. 3.7. The link between DNA damage and chromosome mis-segregation in the *pot1*Δ *pic1-T269* double mutant. (A) The percentage of RPA foci and chromosome mis-segregation in synchronized *pot1*Δ *pic1-T269* cells expressing Rad11 endogenously tagged with mRFP. The cells were culture by incubation at 25°C to obtain log-phase cells, and then cells were synchronized by lactose gradient centrifugation, producing cells at early G2. Synchronized early G2 cells were shifted to 33°C, sampled every 20 min, and monitored for the percentage of RPA foci and chromosome mis-segregation. The time point (0) refers to the synchronized overnight cell culture at 25°C before the temperature shift. The bars refer to the time frame corresponding to early G2, M cells and septated cells (as a marker for S-phase). (B) The percentage of RPA foci in mitotic cells with chromosome mis-segregation 100 and 120 min after temperature shift to 33°C. The scale bar = 5 µm. Examples of cells examined in this experiment are shown on the top. N refers to the total number of cells examined. (C) The percentage of RPA foci in S-phase cells with a septum that display chromosome mis-segregation 100, 120, and 140 min after temperature shift to 33°C.

3.3.6 Neither Shugoshin (Sgo2) nor heterochromatin protein (Swi6) is synthetically lethal with Pot1

The fission yeast has two members of Shugoshin proteins, Sgo1 and Sgo2. The function of Sgo1 is specific to meiosis. However, Sgo2 functions in meiosis and mitosis to ensure proper chromosome segregation [128]. Sgo2 is involved in promoting the centromeric localization of CPC to ensure error-free chromosome segregation. Accordingly, deletion of *sgo2*$^+$ leads to a marked decrease in the centromeric localization of CPC components [129, 130]. Similarly, the heterochromatin protein Swi6 contributes to the loading of the Aurora kinase complex to centromeres in a redundant manner with Sgo2, and *swi6*Δ cells show a reduction in the centromeric localization of CPC [129]. These facts bring a question of whether the deletion of either *sgo2*$^+$ or *swi6*$^+$ is synthetically lethal with Pot1. To explore this possibility, I constructed *pot1*Δ *sgo2*Δ and *pot1*Δ *swi6*Δ double mutants harboring a plasmid expressing *pot1*$^+$ and *tk*$^+$ and examined the ability of the double mutants to survive after the loss of the Pot1 plasmid on FUDR-containing plates using spot assay. Interestingly, I found that both *pot1*Δ *sgo2*Δ and *pot1*Δ *swi6*Δ double mutants could grow after the loss of the Pot1 plasmid (Fig. 3.8A), indicating that *pot1*Δ *sgo2*Δ and *pot1*Δ *swi6*Δ double mutants are not synthetically lethal.

I next confirmed that the *pot1*Δ *sgo2*Δ and the *pot1*Δ *swi6*Δ cells lost the telomeric repeats and harbored circular chromosomes by performing Southern hybridization and PFGE at 30^{o}C as I previously described in the *pot1*Δ *pic1-T269* double mutant. The Southern data indicated the complete loss of telomeric signal (Fig. 3.8B) and PFGE showed that both double mutants carry circular chromosomes like the *pot1*Δ cells (Fig. 3.8C). Collectively, these results imply that the residual centromeric

localization of CPC would be sufficient to maintain the viability of cells with circular chromosomes.

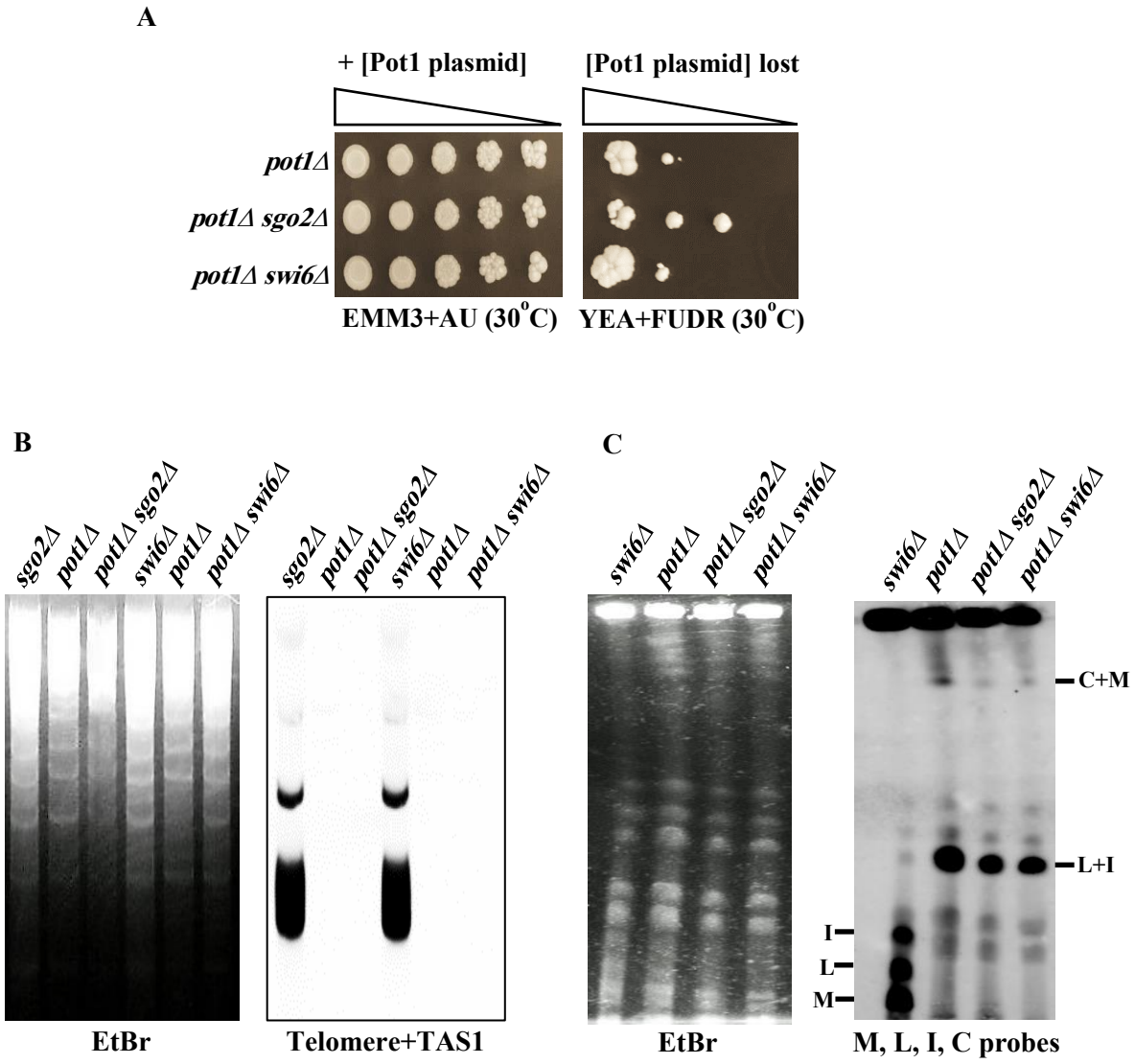

Fig. 3.8. Sgo2 and Swi6 are not synthetically lethal with Pot1. (A) Spot assay of ten-fold serial dilutions of *pot1*Δ, *pot1*Δ *sgo2*Δ and *pot1*Δ *swi6*Δ cells expressing Pot1 plasmid. The plasmid was retained on EMM+AU plates and cells that could grow after the loss of the plasmid were counter-selected on YEA+FUDR at 30°C. (B) The telomere length of the *pot1*Δ *sgo2*Δ and *pot1*Δ *swi6*Δ double mutants was analyzed by Southern hybridization at 30°C. *sgo2*Δ and *swi6*Δ cells are examples for cells with telomeric DNA and *pot1*Δ for cells that lost telomeric repeats. (C) Chromosomal DNA of *swi6*Δ, *pot1*Δ, *pot1*Δ *sgo2*Δ, and *pot1*Δ *swi6*Δ cells were digested with NotI and analyzed by PFGE at 30°C.

3.3.7 *pot1*Δ *sgo2*Δ and *pot1*Δ *swi6*Δ double mutants display a high rate of DNA damage foci but not chromosome mis-segregation

The observation that *pot1*Δ *sgo2*Δ and *pot1*Δ *swi6*Δ double mutants are not synthetically lethal raises a possibility that these double mutants might display lower rates of chromosome mis-segregation and DNA damage compared with the *pot1*Δ *pic1-T269* double mutant. To investigate this possibility, I examined the percentage of chromosome segregation errors and the DNA damage foci in *pot1*Δ *sgo2*Δ and *pot1*Δ *swi6*Δ cells expressing Rad11 endogenously tagged with mRFP. I found that while both *pot1*Δ *sgo2*Δ and *pot1*Δ *swi6*Δ double mutants displayed a high percentage of DNA damage foci, both showed low levels of chromosome mis-segregation compared with that of the *pot1*Δ *pic1-T269* double mutant at 33ºC (Fig. 3.9).

These results point toward the low rates of chromosomes mis-segregation as the reason for the lack of synthetic lethality observed in *pot1*Δ *sgo2*Δ and *pot1*Δ *swi6*Δ double mutants and suggest that the high frequency of chromosome mis-segregation could be the reason for the synthetic lethality observed in *pot1*Δ *pic1-T269* double mutant at 33ºC.

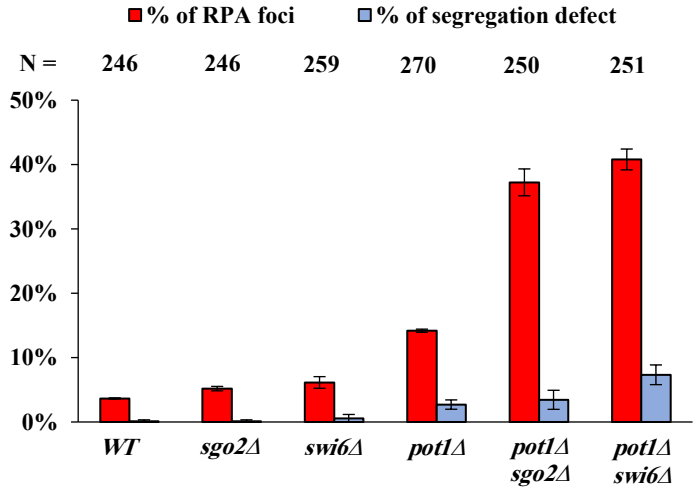

Fig. 3.9. The percentage of RPA foci and chromosome mis-segregation in *WT*, *sgo2*Δ, *swi6*Δ, *pot1*Δ, *pot1*Δ *sgo2*Δ, and *pot1*Δ *swi6*Δ cells expressing Rad11 endogenously-tagged with mRFP were concomitantly counted at 30ºC. (N) in the top indicates the total number of cells examined.

3.4 Summary

In this study, I investigated whether CPC is required for the survival of cells with circular chromosomes using synthetic lethality approach. Throughout this study, I mainly used *pot1*Δ cells as a model strain since deletion of *pot1*$^{+}$ has the advantage of producing cells that can survive only through chromosome circularization. I first examined the synthetic lethality between Pot1 and Cut17/Bir1 and found that *pot1*Δ *cut17-275* and *pot1*Δ *bir1-T1* double mutants failed to grow even at 25ºC (Fig. 3.2), indicating a synthetic lethal interaction between Pot1 and Cut17/Bir1. Since CPC components have an interdependent function [131], it is possible that the other CPC components are also synthetically lethal with Pot1. Indeed, I found that Pot1 is also synthetically lethal with Ark1 and Pic1 (Fig. 3.2).

I further confirmed that this synthetic lethality does not reflect a specific genetic interaction with Pot1 since I found that CPC (Pic1) is also synthetic lethal with *trt1*Δ cells having circular chromosomes (Fig. 3.4D). These results demonstrate that CPC is required for the survival of cells with circular chromosomes in general.

I also observed that inhibiting the function of Pic1 by temperature shift leads to accumulation of elevated rates of chromosome mis-segregation events and DNA damage foci in *pot1*Δ cells (Fig. 3.5C and 3.5D). By analyzing the correlation between the formation of DNA damage and chromosome mis-segregation in the *pot1*Δ *pic1-T269* double mutant, I concluded that first: the DNA damage foci are detected in G2 cells (Fig. 3.7A) and the existence of these foci does not induce chromosome mis-segregation in M-phase (Fig. 3.7B). Second, the generation of DNA damage foci is unlikely to be the outcome of damaging the entrapped mis-segregated chromosomes during cytokinesis (Fig. 3.7C). Third, the generation of DNA damage foci and chromosome mis-segregation are not directly linked. Nevertheless, I do not exclude the

possibility that the DNA damage may be produced later as a consequence of genome instability that arises due to chromosome mis-segregation events.

I next show that the loss-of-function of either Sgo2 or Swi6 does not affect the viability of *pot1*Δ cells (Fig. 3.8A). Further analysis of phenotypes of *pot1*Δ *sgo2*Δ and *pot1*Δ *swi6*Δ double mutants revealed that both double mutants display a high percentage of DNA damage, but both show a markedly low percentage of chromosome mis-segregation compared with that of the *pot1*Δ *pic1-T269* double mutant at 33ºC (Fig. 3.9). This result demonstrates that the chromosome mis-segregation per se but not the DNA damage is the reason for the synthetic lethality of the *pot1*Δ *pic1-T269* double mutant at 33ºC. Also, it further supports the notion that the formation of DNA damage foci is not a direct consequence of chromosome mis-segregation events.

Chapter 4. Conclusions

4.1 Thesis summary

Telomere dysfunction induces genomic instability and promotes carcinogenesis. For instance, recombination-dependent telomere maintenance and chromosome circularization following telomere dysfunction had been reported in association with cancers. In this thesis, I tried to identify vulnerable points in these two telomere dysfunction cases which would help find a possible target for cancer therapy.

Using the genetically tractable organism, fission yeast, I first attempted to understand the mechanism of the TBZ sensitivity phenotype of the *pot1*Δ *rqh1-hd* double mutant which may allow me to find a specific vulnerability in cancer cells that maintain telomeres by HR. Second, I tried to identify a gene required for the maintenance of the circular chromosome using *S. pombe pot1*Δ cells that have a circular chromosome. This gene would be a target of cancer therapy to specifically kill cancer cells harboring circular chromosomes.

In the first study, I have investigated whether there is a link between the long G2 of the *pot1*Δ *rqh1-hd* double mutant and its TBZ sensitivity. I found that shortening the G2 of the *pot1*Δ *rqh1-hd* double mutant by concomitant loss-of-function mutation of Chk1 downstream kinases, Wee1 and Mik1, or gain-of-function mutation of Cdc2 (*cdc2-3w*) suppressed the TBZ sensitivity and the accumulation of recombination intermediates at the telomeres of the double mutant. These results imply that the long G2 is the reason for the TBZ sensitivity of the *pot1*Δ *rqh1-hd* cells in the way that the activation of DNA damage checkpoints and holding the *pot1*Δ *rqh1-hd* cells at long G2 provide cells with time to accumulate recombination structures at telomeres which

disturb chromosomes segregation and render cells sensitive to TBZ. These results further provide insight into the possible roles of DNA damage signaling pathway in the regulation of HR events.

In the second study, I attempted to explore how circular chromosomes are maintained and how cells with circular chromosomes could survive using synthetic lethality approach. By using fission yeast *pot1*Δ and *trt1*Δ cells that have circular chromosomes, I found that the lack of function of CPC components is lethal to cells with circular chromosomes. The lack of functional CPC results in accumulation of elevated rates of chromosomes mis-segregation events and DNA damage. I further found that neither Shugoshin (Sgo2) nor heterochromatin protein (Swi6), which contribute to the centromeric localization of CPC, is lethal to *pot1*Δ cells with circular chromosomes. Both *pot1*Δ *sgo2*Δ and *pot1*Δ *swi6*Δ double mutants show a high percentage of DNA damage but a low percentage of chromosome mis-segregation, suggesting a link between the elevated rates of chromosome mis-segregation and the lethality observed in *pot1*Δ *CPC* double mutants. These results demonstrate the importance of CPC for the survival of cells with circular chromosomes and shed light on the possible role of CPC in the maintenance of circular chromosomes.

4.2 Achievements of the thesis

By using fission yeast *pot1*Δ *rqh1-hd* double mutant that maintains telomeres by HR, a pathway by which some cancer cells can escape telomere loss, I provided a model showing that the activation of DNA damage checkpoint and holding the cells at long G2 could worsen the cell viability rather that enhancing cell survival by contributing to the accumulation of toxic recombination intermediates at the chromosome ends when the telomere function is compromised and render cells sensitive to anti-microtubule drug TBZ. This finding implies that elongation of G2 phase and inhibition of resolution

of recombination intermediate may sensitize cancer cells that maintain telomeres by recombination to anti-microtubule drugs. My results also indicate that not only DNA repair but also DNA damage pathway could contribute to the accumulation of toxic recombination structures at telomeres. Furthermore, my data could provide insight for possible roles of DNA damage protein Chk1 in the regulation of telomere maintenance by the HR pathway through controlling the proteins involved in this pathway.

I further demonstrate the importance of CPC for the survival of cells with circular chromosomes which could provide CPC as a candidate to selectively inhibit the growth of human cancer cells that harbor circular chromosomes. In addition, my observation that accumulation of a high percentage of DNA damage foci in cells with circular chromosomes upon the dysfunction of CPC or the lack of function of proteins that assist in CPC centromeric localization such as Sgo2 or Swi6 suggests a role of the CPC, Sgo2, and Swi6 in the prevention of activation of DNA damage when the chromosomes are circularized, which could be an interesting area to be investigated.

4.3 Future perspectives

In fact, little is known regarding the selective targeting of cancer cells that maintain telomeres through recombination and those harboring circular chromosomes. Fission yeast is an excellent model organism that helps better understand cancer-related phenotypes and develop drug treatment for certain types of cancer.

In this thesis, my data showing that the activation of DNA damage checkpoint and keeping the cells at long G2 unexpectedly worsen the viability of *pot1*Δ *rqh1-hd* double mutant cells in the presence of TBZ could shed light on a possibility to sensitize cancer cells that maintain telomeres by recombination to the anti-microtubule drugs by inhibition of human RecQ helicase and holding the cells at long G2 phase.

Since *pot1*Δ *rqh1-hd* double mutant cells are sensitive to anti-microtubule drug TBZ, *pot1*Δ *rqh1-hd* strain could be exploited in screening for novel microtubule-targeting agents (MTA). MTA constitute a class of drugs that are widely used in cancer therapy. However, the effectiveness of MTA as chemotherapeutic agents has been limited by their adverse side effects such as neurological and hematological side effects. In addition, resistance to many of the existing MTA is another obstacle that impedes the effectiveness of MTA in cancer therapy [132]. Therefore, construction of a drug-sensitive *pot1*Δ *rqh1-hd* strain to screen for novel MTA with fewer side effects and that can avoid the conventional MTA drug resistance would be of clinical outcomes in cancer therapy [133].

Moreover, the observation that deletion of $chk1^{+}$ or its downstream kinase $wee1^{+}$ suppresses the TBZ sensitivity phenotype of the *pot1*Δ *rqh1-hd* cells could provide insight into the possibility of using a drug-sensitive *pot1*Δ *rqh1-hd* strain for the positive screening of Chk1 or Wee1 inhibitors (chemical compounds that could inhibit Chk1 or Wee1 would suppress the TBZ sensitivity of *pot1*Δ *rqh1-hd* cells). Cancer cells with no functional G1 checkpoint rely mainly on the G2/M checkpoint, mediated by Chk1 and Wee1, for cell survival. Therefore, abrogation of the G2/M checkpoint by inhibiting the function of Chk1 or Wee1 despite the presence of DNA damage can lead to mitotic catastrophe and cell death and hence selectively sensitize the G1 defective cancer cells to DNA damaging agents [134].

On the side of chromosome circularization, besides the evaluation of the possibility to kill human cancer cells having ring chromosomes by targeting CPC, investigating the reason behind the accumulation of high levels of DNA damage foci in cells harboring circular chromosomes upon the lack of function of CPC or reduction of its centromeric localization would provide insight into novel roles of CPC in the

prevention of DNA damage upon chromosome circularization. Moreover, developing a drug-sensitive *pot1*Δ strain may greatly assist in identifying the genes required for the survival of cells having circular chromosomes using the chemical-genetic screen [133, 135]. This screen is based on the idea to find the chemical compounds that can selectively inhibit the growth of cells harboring circular chromosomes (e.g., *pot1*Δ cells), but not linear ones. Identifying the target of these compounds would provide insight about the genes required for the maintenance of circular chromosomes which would be of clinical implications in selective killing of human cancer cells that harbor circular chromosomes.

References

[1] Muller HJ. The remaking of chromosomes. Collecting net. 1938;13:181-98.

[2] McClintock B. The stability of broken ends of chromosomes in *Zea mays*. Genetics. 1941;26(2):234-82.

[3] Blackburn EH, Gall JG. A tandemly repeated sequence at the termini of the extrachromosomal ribosomal RNA genes in *Tetrahymena*. Journal of molecular biology. 1978;120(1):33-53.

[4] Szostak JW, Blackburn EH. Cloning yeast telomeres on linear plasmid vectors. Cell. 1982;29(1):245-55.

[5] Varela E, Blasco M. 2009 Nobel Prize in Physiology or Medicine: telomeres and telomerase. Oncogene. 2010;29(11):1561.

[6] Blackburn EH. Switching and signaling at the telomere. Cell. 2001;106(6):661-73.

[7] Makarov VL, Hirose Y, Langmore JP. Long G tails at both ends of human chromosomes suggest a C strand degradation mechanism for telomere shortening. Cell. 1997;88(5):657-66.

[8] Samassekou O, Gadji M, Drouin R, Yan J. Sizing the ends: normal length of human telomeres. Annals of Anatomy-Anatomischer Anzeiger. 2010;192(5):284-91.

[9] Sugawara NF. DNA sequences at the telomeres of the fission yeast *S. pombe*. Ph.D. thesis, Harvard University. 1988.

[10] Wang S, Zakian VA. Sequencing of *Saccharomyces* telomeres cloned using T4 DNA polymerase reveals two domains. Molecular and cellular biology. 1990;10(8):4415-9.

[11] Prowse KR, Greider CW. Developmental and tissue-specific regulation of mouse telomerase and telomere length. Proceedings of the National Academy of Sciences. 1995;92(11):4818-22.

[12] Biessmann H, Carter SB, Mason JM. Chromosome ends in *Drosophila* without telomeric DNA sequences. Proceedings of the National Academy of Sciences. 1990;87(5):1758-61.

[13] Meyne J, Ratliff RL, Moyzis RK. Conservation of the human telomere sequence (TTAGGG) n among vertebrates. Proceedings of the National Academy of Sciences. 1989;86(18):7049-53.

[14] Greider CW, Blackburn EH. A telomeric sequence in the RNA of *Tetrahymena* telomerase required for telomere repeat synthesis. Nature. 1989;337(6205):331.

[15] Smith FW, Feigon J. Quadruplex structure of *Oxytricha* telomeric DNA oligonucleotides. Nature. 1992;356(6365):164.

[16] McKnight T, Fitzgerald M, Shippen D. Plant telomeres and telomerases. A review. Biochemistry-New York-English Translation of Biokhimiya. 1997;62(11):1224-31.

[17] Petracek ME, Lefebvre PA, Silflow CD, Berman J. *Chlamydomonas* telomere sequences are A+ T-rich but contain three consecutive GC base pairs. Proceedings of the National Academy of Sciences. 1990;87(21):8222-6.

[18] Okazaki R, Okazaki T, Sakabe K, Sugimoto K, Sugino A. Mechanism of DNA chain growth. I. Possible discontinuity and unusual secondary structure of newly synthesized chains. Proceedings of the National Academy of Sciences. 1968;59(2):598-605.

[19] Watson JD. Origin of concatemeric T7 DNA. Nature New Biology. 1972;239(94):197.

[20] Olovnikov AM. A theory of marginotomy: the incomplete copying of template margin in enzymic synthesis of polynucleotides and biological significance of the phenomenon. Journal of theoretical biology. 1973;41(1):181-90.

[21] Maciejowski J, de Lange T. Telomeres in cancer: tumour suppression and genome instability. Nature reviews Molecular cell biology. 2017;18(3):175.

[22] Hayflick L. The limited in vitro lifetime of human diploid cell strains. Experimental cell research. 1965;37(3):614-36.

[23] Reaper PM, Fagagna FdAd, Jackson SP. Activation of the DNA damage response by telomere attrition: a passage to cellular senescence. Cell Cycle. 2004;3(5):541-4.

[24] De Lange T. Shelterin: the protein complex that shapes and safeguards human telomeres. Genes & development. 2005;19(18):2100-10.

[25] Jain D, Cooper JP. Telomeric strategies: means to an end. Annual review of genetics. 2010;44:243-69.

[26] Broccoli D, Smogorzewska A, Chong L, de Lange T. Human telomeres contain two distinct Myb–related proteins, TRF1 and TRF2. Nature genetics. 1997;17(2):231.

[27] Lei M, Podell ER, Cech TR. Structure of human POT1 bound to telomeric single-stranded DNA provides a model for chromosome end-protection. Nature Structural and Molecular Biology. 2004;11(12):1223.

[28] Ye JZ-S, Hockemeyer D, Krutchinsky AN, Loayza D, Hooper SM, Chait BT, et al. POT1-interacting protein PIP1: a telomere length regulator that recruits POT1 to the TIN2/TRF1 complex. Genes & development. 2004;18(14):1649-54.

[29] Cooper JP, Nimmo ER, Allshire RC, Cech TR. Regulation of telomere length and function by a Myb-domain protein in fission yeast. Nature. 1997;385(6618):744-7.

[30] Baumann P, Cech TR. Pot1, the putative telomere end-binding protein in fission yeast and humans. Science. 2001;292(5519):1171-5.

[31] Miyoshi T, Kanoh J, Saito M, Ishikawa F. Fission yeast Pot1-Tpp1 protects telomeres and regulates telomere length. Science. 2008;320(5881):1341-4.

[32] Miller KM, Rog O, Cooper JP. Semi-conservative DNA replication through telomeres requires Taz1. Nature. 2006;440(7085):824.

[33] Robles-Espinoza CD, Harland M, Ramsay AJ, Aoude LG, Quesada V, Ding Z, et al. POT1 loss-of-function variants predispose to familial melanoma. Nature genetics. 2014;46(5):478.

[34] Calvete O, Martinez P, Garcia-Pavia P, Benitez-Buelga C, Paumard-Hernández B, Fernandez V, et al. A mutation in the POT1 gene is responsible for cardiac angiosarcoma in TP53-negative Li–Fraumeni-like families. Nature communications. 2015;6:8383.

[35] Chang S. Cancer chromosomes going to POT1. Nature genetics. 2013;45(5):473.

[36] Shay J, Bacchetti S. A survey of telomerase activity in human cancer. European journal of cancer. 1997;33(5):787-91.

[37] Bryan TM, Englezou A, Dalla-Pozza L, Dunham MA, Reddel RR. Evidence for an alternative mechanism for maintaining telomere length in human tumors and tumor-derived cell lines. Nature medicine. 1997;3(11):1271.

[38] Roth CW, Kobeski F, Walter MF, Biessmann H. Chromosome end elongation by recombination in the mosquito *Anopheles gambiae*. Molecular and Cellular Biology. 1997;17(9):5176-83.

[39] Lundblad V, Blackburn EH. An alternative pathway for yeast telomere maintenance rescues est1− senescence. Cell. 1993;73(2):347-60.

[40] Nakamura TM, Cooper JP, Cech TR. Two modes of survival of fission yeast without telomerase. Science. 1998;282(5388):493-6.

[41] Niida H, Shinkai Y, Hande MP, Matsumoto T, Takehara S, Tachibana M, et al. Telomere maintenance in telomerase-deficient mouse embryonic stem cells: characterization of an amplified telomeric DNA. Molecular and cellular biology. 2000;20(11):4115-27.

[42] Lichtsteiner SP, Lebkowski JS, Vasserot AP. Telomerase: a target for anticancer therapy. Annals of the New York Academy of Sciences. 1999;886(1):1-11.

[43] Croteau DL, Popuri V, Opresko PL, Bohr VA. Human RecQ helicases in DNA repair, recombination, and replication. Annual review of biochemistry. 2014;83:519-52.

[44] Stewart E, Chapman CR, Al-Khodairy F, Carr AM, Enoch T. rqh1+, a fission yeast gene related to the Bloom's and Werner's syndrome genes, is required for reversible S phase arrest. The EMBO Journal. 1997;16(10):2682-92.

[45] Gangloff S, McDonald JP, Bendixen C, Arthur L, Rothstein R. The yeast type I topoisomerase Top3 interacts with Sgs1, a DNA helicase homolog: a potential eukaryotic reverse gyrase. Molecular and cellular biology. 1994;14(12):8391-8.

[46] Hanada K, Hickson I. Molecular genetics of RecQ helicase disorders. Cellular and molecular life sciences. 2007;64(17):2306-22.

[47] Cohen H, Sinclair DA. Recombination-mediated lengthening of terminal telomeric repeats requires the Sgs1 DNA helicase. Proceedings of the National Academy of Sciences. 2001;98(6):3174-9.

[48] Stavropoulos DJ, Bradshaw PS, Li X, Pasic I, Truong K, Ikura M, et al. The Bloom syndrome helicase BLM interacts with TRF2 in ALT cells and promotes telomeric DNA synthesis. Human molecular genetics. 2002;11(25):3135-44.

[49] Opresko PL, Otterlei M, Graakjær J, Bruheim P, Dawut L, Kølvraa S, et al. The Werner syndrome helicase and exonuclease cooperate to resolve telomeric D loops in a manner regulated by TRF1 and TRF2. Molecular cell. 2004;14(6):763-74.

[50] Wang X, Baumann P. Chromosome fusions following telomere loss are mediated by single-strand annealing. Molecular cell. 2008;31(4):463-73.

[51] Takahashi K, Imano R, Kibe T, Seimiya H, Muramatsu Y, Kawabata N, et al. Fission yeast Pot1 and RecQ helicase are required for efficient chromosome segregation. Molecular and cellular biology. 2011;31(3):495-506.

[52] Cote G, Katsantoni A, Deligeorgis D. The cytogenetic and clinical implications of a ring chromosome 2. Ann Genet. 1981;24(4):231-5.

[53] Guilherme RS, Meloni VFA, Kim CA, Pellegrino R, Takeno SS, Spinner NB, et al. Mechanisms of ring chromosome formation, ring instability and clinical consequences. BMC medical genetics. 2011;12(1):171.

[54] Bolzán AD. Chromosomal aberrations involving telomeres and interstitial telomeric sequences. Mutagenesis. 2011;27(1):1-15.

[55] Yip M-Y. Autosomal ring chromosomes in human genetic disorders. Translational pediatrics. 2015;4(2):164.

[56] Morgan LV. Correlation between shape and behavior of a chromosome. Proceedings of the National Academy of Sciences. 1926;12(3):180-1.

[57] McClintock B. A correlation of ring-shaped chromosomes with variegation in *Zea mays*. Proceedings of the National Academy of Sciences. 1932;18(12):677-81.

[58] Kosztolányi G. The genetics and clinical characteristics of constitutional ring chromosomes. J Assoc Genet Technol. 2009;35(2):44-8.

[59] Ledbetter D, Riccardi V, Au W, Wilson D, Holmquist G. Ring chromosome 15: phenotype, Ag-NOR analysis, secondary aneuploidy, and associated chromosome instability. Cytogenetic and Genome Research. 1980;27(2-3):111-22.

[60] Kosztolányi G. Does “ring syndrome” exist? An analysis of 207 case reports on patients with a ring autosome. Human genetics. 1987;75(2):174-9.

[61] Elens I, Vanrykel K, De Waele L, Jansen K, Segeren M, Van Paesschen W, et al. Ring chromosome 20 syndrome: electroclinical description of six patients and review of the literature. Epilepsy & Behavior. 2012;23(4):409-14.

[62] Gebhart E. Ring chromosomes in human neoplasias. Cytogenetic and genome research. 2008;121(3-4):149-73.

[63] Cho EH, Park JB, Kim JK. Atypical teratoid rhabdoid brain tumor in an infant with ring chromosome 22. Korean journal of pediatrics. 2014;57(7):333-6.

[64] Nilbert M, Mitelman F, Mandahl N, Rydholm A, Willén H. MDM2 gene amplification correlates with ring chromosomes in soft tissue tumors. Genes, Chromosomes and Cancer. 1994;9(4):261-5.

[65] Labropoulos SV, Razis ED. Imatinib in the treatment of dermatofibrosarcoma protuberans. Biologics: targets & therapy. 2007;1(4):347.

[66] Kim T, Bershteyn M, Wynshaw-Boris A. Chromosome therapy: correction of large chromosomal aberrations by inducing ring chromosomes in induced pluripotent stem cells (iPSCs). Nucleus. 2014;5(5):391-5.

[67] Bershteyn M, Hayashi Y, Desachy G, Hsiao EC, Sami S, Tsang KM, et al. Cell-autonomous correction of ring chromosomes in human induced pluripotent stem cells. Nature. 2014;507(7490):99.

[68] Heckman DS, Geiser DM, Eidell BR, Stauffer RL, Kardos NL, Hedges SB. Molecular evidence for the early colonization of land by fungi and plants. Science. 2001;293(5532):1129-33.

[69] Hedges SB. The origin and evolution of model organisms. Nature Reviews Genetics. 2002;3(11):838.

[70] Lindner P. *Schizosaccharomyces pombe* n. sp., ein neuer Gährungserreger. Wochenschrift für Brauerei. 1893;10:1298-300.

[71] Leupold U. Die Vererbung von Homothallie und Heterothallie bei *Schizosaccharomyces pombe*. CR Lab Carlsberg Sér Physiol. 1950;24: 381–480.

[72] Leupold U. The origin of *Schizosaccharomyces pombe* genetics. The early days of yeast genetics. 1993:125-8.

[73] Hayles J, Nurse P. Introduction to Fission Yeast as a Model System. Cold Spring Harbor Protocols. 2018;2018(5):pdb. top079749.

[74] Krawchuk MD, Wahls WP. High-efficiency gene targeting in *Schizosaccharomyces pombe* using a modular, PCR-based approach with long tracts of flanking homology. Yeast (Chichester, England). 1999;15(13):1419.

[75] Petersen J, Russell P. Growth and the environment of *Schizosaccharomyces pombe*. Cold Spring Harbor Protocols. 2016;2016(3):pdb. top079764.

[76] Yamashita A, Sakuno T, Watanabe Y, Yamamoto M. Analysis of *Schizosaccharomyces pombe* meiosis. Cold Spring Harbor Protocols. 2017;2017(9):pdb. top079855.

[77] Ding R, West RR, Morphew D, Oakley BR, McIntosh J. The spindle pole body of *Schizosaccharomyces pombe* enters and leaves the nuclear envelope as the cell cycle proceeds. Molecular biology of the cell. 1997;8(8):1461-79.

[78] Goffeau A, Aert R, Agostini-Carbone M, Ahmed A, Aigle M, Alberghina L, et al. The yeast genome directory. Nature. 1997;387(6632):5-6.

[79] Consortium TCeS. Genome sequence of the nematode *C. elegans*: a platform for investigating biology. Science. 1998:2012-8.

[80] Adams MD, Celniker SE, Holt RA, Evans CA, Gocayne JD, Amanatides PG, et al. The genome sequence of *Drosophila melanogaster*. Science. 2000;287(5461):2185-95.

[81] Initiative AG. Analysis of the genome sequence of the flowering plant *Arabidopsis thaliana*. Nature. 2000;408(6814):796.

[82] Venter JC, Adams MD, Myers EW, Li PW, Mural RJ, Sutton GG, et al. The sequence of the human genome. Science. 2001;291(5507):1304-51.

[83] Wood V, Gwilliam R, Rajandream M-A, Lyne M, Lyne R, Stewart A, et al. The genome sequence of *Schizosaccharomyces pombe*. Nature. 2002;415(6874):871.

[84] Habib AG, Masuda K, Yukawa M, Tsuchiya E, Ueno M. Long G2 accumulates recombination intermediates and disturbs chromosome segregation at dysfunction telomere in *Schizosaccharomyces pombe*. Biochemical and biophysical research communications. 2015;464(1):140-6.

[85] Hartwell LH, Weinert TA. Checkpoints: controls that ensure the order of cell cycle events. Science. 1989;246(4930):629-34.

[86] Elledge SJ. Cell cycle checkpoints: preventing an identity crisis. Science. 1996;274(5293):1664-72.

[87] Hartwell LH, Kastan MB. Cell cycle control and cancer. Science. 1994;266(5192):1821-8.

[88] O'Connell MJ, Raleigh JM, Verkade HM, Nurse P. Chk1 is a wee1 kinase in the G2 DNA damage checkpoint inhibiting cdc2 by Y15 phosphorylation. The EMBO journal. 1997;16(3):545-54.

[89] Walworth N, Davey S, Beach D. Fission yeast chkl protein kinase links the rad checkpoint pathway to cdc2. Nature. 1993;363(6427):368.

[90] Al-Khodairy F, Fotou E, Sheldrick K, Griffiths D, Lehmann AR, Carr A. Identification and characterization of new elements involved in checkpoint and feedback controls in fission yeast. Molecular Biology of the Cell. 1994;5(2):147-60.

[91] Walworth NC, Bernards R. rad-dependent response of the chk1-encoded protein kinase at the DNA damage checkpoint. Science. 1996;271(5247):353-6.

[92] Rhind N, Russell P. Roles of the mitotic inhibitors Wee1 and Mik1 in the G2 DNA damage and replication checkpoints. Molecular and cellular biology. 2001;21(5):1499-508.

[93] Lundgren K, Walworth N, Booher R, Dembski M, Kirschner M, Beach D. mik1 and wee1 cooperate in the inhibitory tyrosine phosphorylation of cdc2. Cell. 1991;64(6):1111-22.

[94] Nurse P. Universal control mechanism regulating onset of M-phase. Nature. 1990;344(6266):503.

[95] Lew DJ, Kornbluth S. Regulatory roles of cyclin dependent kinase phosphorylation in cell cycle control. Current opinion in cell biology. 1996;8(6):795-804.

[96] Russell P, Nurse P. cdc25+ functions as an inducer in the mitotic control of fission yeast. Cell. 1986;45(1):145-53.

[97] Nakano A, Masuda K, Hiromoto T, Takahashi K, Matsumoto Y, Habib AG, et al. Rad51-dependent aberrant chromosome structures at telomeres and ribosomal DNA activate the spindle assembly checkpoint. Molecular and cellular biology. 2014;34(8):1389-97.

[98] Fantes PA. Isolation of cell size mutants of a fission yeast by a new selective method: characterization of mutants and implications for division control mechanisms. Journal of bacteriology. 1981;146(2):746-54.

[99] Churikov D, Price CM. Pot1 and cell cycle progression cooperate in telomere length regulation. Nature Structural and Molecular Biology. 2008;15(1):79.

[100] Wu L, Multani AS, He H, Cosme-Blanco W, Deng Y, Deng JM, et al. Pot1 deficiency initiates DNA damage checkpoint activation and aberrant homologous recombination at telomeres. Cell. 2006;126(1):49-62.

[101] Maftahi M, Hope JC, Delgado-Cruzata L, Han CS, Freyer GA. The severe slow growth of *Δ srs2 Δ rqh1* in *Schizosaccharomyces pombe* is suppressed by loss of recombination and checkpoint genes. Nucleic acids research. 2002;30(21):4781-92.

[102] Habib AG, Sugiura K, Ueno M. Chromosome passenger complex is required for the survival of cells with ring chromosomes in fission yeast. PloS one. 2018;13(1):e0190523.

[103] Naito T, Matsuura A, Ishikawa F. Circular chromosome formation in a fission yeast mutant defective in two ATM homologues. Nature genetics. 1998;20(2):203.

[104] Kaelin Jr WG. The concept of synthetic lethality in the context of anticancer therapy. Nature reviews cancer. 2005;5(9):689.

[105] Vagnarelli P, Earnshaw WC. Chromosomal passengers: the four-dimensional regulation of mitotic events. Chromosoma. 2004;113(5):211-22.

[106] Earnshaw WC, Bernat RL. Chromosomal passengers: toward an integrated view of mitosis. Chromosoma. 1991;100(3):139-46.

[107] van der Horst A, Lens SM. Cell division: control of the chromosomal passenger complex in time and space. Chromosoma. 2014;123(1-2):25-42.

[108] Bohnert KA, Chen J-S, Clifford DM, Vander Kooi CW, Gould KL. A link between aurora kinase and Clp1/Cdc14 regulation uncovered by the identification of a fission yeast borealin-like protein. Molecular biology of the cell. 2009;20(16):3646-59.

[109] Leverson JD, Huang H-k, Forsburg SL, Hunter T. The *Schizosaccharomyces pombe* aurora–related kinase Ark1 interacts with the inner centromere protein Pic1 and mediates chromosome segregation and cytokinesis. Molecular biology of the cell. 2002;13(4):1132-43.

[110] Sen S, Zhou H, White RA. A putative serine/threonine kinase encoding gene BTAK on chromosome 20q13 is amplified and overexpressed in human breast cancer cell lines. Oncogene. 1997;14(18):2195.

[111] Bischoff JR, Anderson L, Zhu Y, Mossie K, Ng L, Souza B, et al. A homologue of *Drosophila* aurora kinase is oncogenic and amplified in human colorectal cancers. The EMBO journal. 1998;17(11):3052-65.

[112] Sorrentino R, Libertini S, Pallante PL, Troncone G, Palombini L, Bavetsias V, et al. Aurora B overexpression associates with the thyroid carcinoma undifferentiated phenotype and is required for thyroid carcinoma cell proliferation. The Journal of Clinical Endocrinology & Metabolism. 2005;90(2):928-35.

[113] Lin Z-Z, Jeng Y-M, Hu F-C, Pan H-W, Tsao H-W, Lai P-L, et al. Significance of Aurora B overexpression in hepatocellular carcinoma. Aurora B Overexpression in HCC. BMC cancer. 2010;10(1):461.

[114] Smith S, Bowers N, Betticher D, Gautschi O, Ratschiller D, Hoban P, et al. Overexpression of aurora B kinase (AURKB) in primary non-small cell lung carcinoma is frequent, generally driven from one allele, and correlates with the level of genetic instability. British journal of cancer. 2005;93(6):719.

[115] Kapellos G, Polonifi K, Farmakis D, Spartalis E, Tomos P, Aessopos A, et al. Overexpression of survivin levels in circulation and tissue samples of lung cancer patients. Anticancer research. 2013;33(8):3475-80.

[116] Chen W-C, Liu Q, Fu J-X, Kang S-Y. Expression of survivin and its significance in colorectal cancer. World Journal of Gastroenterology: WJG. 2004;10(19):2886.

[117] Nassar A, Sexton D, Cotsonis G, Cohen C. Survivin expression in breast carcinoma: correlation with apoptosis and prognosis. Applied Immunohistochemistry & Molecular Morphology. 2008;16(3):221-6.

[118] Kishi H, Igawa M, Kikuno N, Yoshino T, Urakami S, Shiina H. Expression of the survivin gene in prostate cancer: correlation with clinicopathological characteristics, proliferative activity and apoptosis. The Journal of urology. 2004;171(5):1855-60.

[119] Yamada Y, Kuroiwa T, Nakagawa T, Kajimoto Y, Dohi T, Azuma H, et al. Transcriptional expression of survivin and its splice variants in brain tumors in humans. Journal of neurosurgery. 2003;99(4):738-45.

[120] Ikeguchi M, Ueda T, Sakatani T, Hirooka Y, Kaibara N. Expression of survivin messenger RNA correlates with poor prognosis in patients with hepatocellular carcinoma. Diagnostic Molecular Pathology. 2002;11(1):33-40.

[121] Chen Y-J, Chen C-M, Twu N-F, Yen M-S, Lai C-R, Wu H-H, et al. Overexpression of Aurora B is associated with poor prognosis in epithelial ovarian cancer patients. Virchows Archiv. 2009;455(5):431.

[122] Garg H, Suri P, Gupta JC, Talwar G, Dubey S. Survivin: a unique target for tumor therapy. Cancer cell international. 2016;16(1):49.

[123] Kollareddy M, Zheleva D, Dzubak P, Brahmkshatriya PS, Lepsik M, Hajduch M. Aurora kinase inhibitors: progress towards the clinic. Investigational new drugs. 2012;30(6):2411-32.

[124] Sclafani RA, Fangman WL. Thymidine utilization by *tut* mutants and facile cloning of mutant alleles by plasmid conversion in *S. cerevisiae*. Genetics. 1986;114(3):753-67.

[125] Janssen A, van der Burg M, Szuhai K, Kops GJ, Medema RH. Chromosome segregation errors as a cause of DNA damage and structural chromosome aberrations. Science. 2011;333(6051):1895-8.

[126] Santaguida S, Amon A. Short-and long-term effects of chromosome mis-segregation and aneuploidy. Nature reviews Molecular cell biology. 2015;16(8):473.

[127] Iftode C, Daniely Y, Borowiec JA. Replication protein A (RPA): the eukaryotic SSB. Critical reviews in biochemistry and molecular biology. 1999;34(3):141-80.

[128] Kitajima TS, Kawashima SA, Watanabe Y. The conserved kinetochore protein shugoshin protects centromeric cohesion during meiosis. Nature. 2004;427(6974):510.

[129] Kawashima SA, Tsukahara T, Langegger M, Hauf S, Kitajima TS, Watanabe Y. Shugoshin enables tension-generating attachment of kinetochores by loading Aurora to centromeres. Genes & development. 2007;21(4):420-35.

[130] Vanoosthuyse V, Prykhozhij S, Hardwick KG. Shugoshin 2 regulates localization of the chromosomal passenger proteins in fission yeast mitosis. Molecular biology of the cell. 2007;18(5):1657-69.

[131] Kaitna S, Mendoza M, Jantsch-Plunger V, Glotzer M. Incenp and an Aurora-like kinase form a complex essential for chromosome segregation and efficient completion of cytokinesis. Current Biology. 2000;10(19):1172-81.

[132] Zhou J, Giannakakou P. Targeting microtubules for cancer chemotherapy. Current Medicinal Chemistry-Anti-Cancer Agents. 2005;5(1):65-71.

[133] Kawashima SA, Takemoto A, Nurse P, Kapoor TM. Analyzing fission yeast multidrug resistance mechanisms to develop a genetically tractable model system for chemical biology. Chemistry & biology. 2012;19(7):893-901.

[134] Benada J, Macurek L. Targeting the checkpoint to kill cancer cells. Biomolecules. 2015;5(3):1912-37.

[135] Wong LH, Unciti-Broceta A, Spitzer M, White R, Tyers M, Harrington L. A yeast chemical genetic screen identifies inhibitors of human telomerase. Chemistry & biology. 2013;20(3):333-40.

Acknowledgments

First and foremost, I would like to express my sincere gratitude to my academic supervisor Dr. Masaru Ueno for his motivation, guidance, continuous support, and invaluable insights and suggestions to improve my writing of the thesis and my Ph.D. work in general. It was a great privilege and honor to perform my master and doctoral work under his supervision and to learn from his immense research expertise.

My sincere thanks to Dr. Seiji Kawamoto, Dr. Nobukazu Tanaka and Dr. Tsunehiro Aki for investing their time to revise my Ph.D. thesis and providing me with insightful comments that shaped my final dissertation.

I am also extremely grateful to the Ministry of Education, Culture, Sports, Science and Technology (MEXT), Japan for providing me with a scholarship to pursue my master and Ph.D. degree in Hiroshima University.

I would like to express my deepest thanks to all staff members of the student support office in the Graduate School of Advanced Sciences of Matter for their generous help throughout my study at Hiroshima University. I am also deeply grateful to the Graduate School of Advanced Sciences of Matter for the generous fund and support to attend several international scientific meetings during my study.

I would like to express special thanks and deep gratitude to my parents for their endless love, encouragement, sacrifices, and support of my academic life and my life in general.

Finally, but by no means least, my heartfelt thanks to my friends and to everyone who supported me throughout my life and my study to make this thesis possible.

Ahmed Gamal Kamel Habib